OPTIMAL ERROR ESTIMATES OF A LOW-REGULARITY INTEGRATOR FOR THE SQG EQUATIONS UNDER ENDPOINT REGULARITY

XINYU CHENG, ZHAONAN LUO, AND SHENG WANG

Abstract. We propose and analyze a novel semi-implicit low-regularity integrator (LRI) for the dissipative surface quasi-geostrophic (SQG) equations. The semi-implicit treatment yields an exact discrete transport cancellation and hence unconditional energy stability, while retaining the efficiency of an exponential treatment of the fractional dissipation. To overcome the suboptimal regularity requirements typical of standard Sobolev-based error analysis for active scalars, we introduce a general numerical Besov space framework. Within this framework, we establish a sharp $B^0_{\infty,1}$-error estimate and prove first-order temporal convergence under the endpoint assumption $\theta \in L^\infty(0,T;B^2_{\infty,1})$. The gain is the removal of the additional fractional derivative loss in the Sobolev analysis; it is not an inclusion-wise weakening of the $W^{2,2+\epsilon}$ assumption. We present rigorous proofs for the stability and error bounds, complemented by extensive numerical experiments including convergence tests, vanishing viscosity limit validations, and complex vortex dynamics, to demonstrate the robustness and accuracy of the method under low-regularity conditions.

1. Introduction

1.1. The SQG Model. This paper focuses on the sharp numerical approximation of the dissipative surface quasi-geostrophic (SQG) equations for the active scalar field $\theta : \mathbb{T}^2 \times [0,\infty) \to \mathbb{R}$:

$$\begin{cases} \partial_t \theta + u \cdot \nabla \theta = -\nu \Lambda^\gamma \theta, \\ u = \nabla^\perp \Lambda^{-1}\theta = (-\partial_2 \Lambda^{-1}\theta, \partial_1 \Lambda^{-1}\theta), \\ \theta|_{t=0} = \theta_0, \end{cases} \tag{SQG}$$

where $\nu \geq 0$ is the viscosity, $0 < \gamma \leq 2$ is the fractional dissipation parameter, and $\mathbb{T}^2 = [-\pi,\pi]^2$. The unknown θ represents the potential temperature in geophysical fluid dynamics (Pedlosky, 1982; Held et al., 1995). The (SQG) system models the temperature evolution in a rapidly rotating stratified fluid and can be derived from the 3D Boussinesq equations (Pedlosky, 1982). The operator $\Lambda = (-\Delta)^{\frac{1}{2}}$ is the fractional Laplacian. The well-posedness of the (SQG) equations has been extensively studied; see, for example, Resnick (1995) and Marchand (2008). Further analytical results on global weak solutions, global existence for related nonlocal transport equations, and nonuniqueness of weak SQG solutions can be found in (Bae and Granero-Belinchón, 2015; Constantin and Nguyen, 2018; Buckmaster et al., 2019; Cheng et al., 2021; Isett and Ma, 2021).

1.2. Semi-Implicit Low-Regularity Integrator (LRI). Solving the SQG equations numerically presents profound challenges due to the highly singular and nonlocal nature of the velocity field $u = \nabla^\perp \Lambda^{-1}\theta$. Classical explicit methods often require stringent stability restrictions, while fully implicit methods can be computationally prohibitive. On the other hand, regarding energy conservation, Onsager conjectured in 1949 that a loss of regularity may lead to "anomalous energy dissipation" or "energy cascades". Therefore, computing such "rough" solutions is of profound physical and mathematical significance. To effectively handle the nonlocal fractional dissipation and the singular convection term without artificially inflating the regularity assumptions, we propose the following first-order semi-implicit low-regularity integrator (LRI), based on an exponential integrator, for the SQG equations:

$$\begin{cases} \theta^{n+1} + \tau(e^{-\nu\tau\Lambda^\gamma} u^n \cdot \nabla\theta^{n+1}) = e^{-\nu\tau\Lambda^\gamma}\theta^n, \\ u^n = \nabla^\perp \Lambda^{-1}\theta^n, \\ \theta^0 = \theta_0, \end{cases} \tag{1.1}$$

where τ is the time step size. Induction verifies that the zero-mean property $\int_{\mathbb{T}^2} \theta^n \, dx = 0$ and the incompressibility $\nabla \cdot u^n = 0$ are perfectly preserved at the discrete level.

The semi-implicit treatment of the transport term is essential to the stability mechanism. Since $e^{-\nu\tau\Lambda^\gamma} u^n$ is divergence free, testing (1.1) by θ^{n+1} cancels the transport contribution exactly and gives the unconditional L^2 estimate in Proposition 1.1. The method requires only a linear solve at each step, implemented by the fixed-point iteration in (A.5). By contrast, replacing θ^{n+1} in the transport term by θ^n destroys this discrete cancellation. An explicit exponential method can still be analyzed by related consistency estimates, but its stability estimate generally requires a time-step restriction (and, after spatial discretization, a CFL-type coupling with the Fourier cut-off). Thus the present argument does not yield a comparable unconditional error bound for the explicit variant.

1.3. **Historical Review and Motivation.** Numerical simulations of active scalars and incompressible fluids, including the SQG equations, have been extensively explored using classical techniques such as finite difference method (Chorin, 1968; Wetton, 2006), finite element method (Heywood and Rannacher, 1982, 1990; Hill and Süli, 2000), spectral method (Guo and Zou, 2003), the Lagrange-Galerkin method (He, 2013; Süli, 1988), and projection method (Chorin, 1969; Hou and Wetton, 1993; E and Liu, 1995). For the SQG equations specifically, numerical simulations on periodic domains and various boundary conditions were elegantly conducted by Bonito and Nazarov (2021) and Constantin et al. (2012). More recently, neural network methods have also been introduced to approximate SQG dynamics (Abdo et al., 2025), following seminal machine learning techniques for fluids (Han et al., 2018).

Despite these advancements, classical numerical methods for active scalars typically require high regularity assumptions to achieve optimal convergence rates. Recently, low-regularity methods for numerical computation of fluid models have seen vigorous development, significantly relaxing regularity requirements compared to classical schemes (Bai et al., 2023; Cao et al., 2025; Rousset and Schratz, 2021; Wu and Zhao, 2022). Notably, Li, Ma, and Schratz (2022) developed an elegant semi-implicit exponential integrator for the Navier–Stokes equations, lowering the regularity requirements significantly. However, standard numerical analysis techniques for these advanced schemes rely heavily on Sobolev spaces (H^s). As observed in the literature, Sobolev-based error analysis for quasi-linear active scalars suffers from severe derivative loss when bounding the highly singular nonlocal convection term. Consequently, obtaining a first-order temporal convergence typically requires the exact solution to be bounded in $W^{2,2+\epsilon}(\mathbb{T}^2)$ or $H^{2+\delta}(\mathbb{T}^2)$ for some $\delta > 0$, which strictly demands more than two spatial derivatives.

1.4. **Introduction to the Numerical Besov Framework.** For the SQG equations, where anomalous dissipation and rough fronts (e.g., vortex patches) are physical hallmarks, assuming $H^{2+\delta}$ regularity is often overly restrictive. The fundamental mathematical obstacle is that standard Kato-Ponce type energy estimates in Sobolev spaces suffer from derivative loss when bounding the nonlinear convection term, thereby forcing an artificial increment in the required Sobolev index.

To fundamentally break this barrier, we introduce a *numerical Besov space framework* for active scalars and general fluid models as the primary contribution of this paper. By transitioning from the classical Sobolev space L^2 to the critically embedded Besov space $B^0_{\infty,1}$, we leverage specific product rules (div-curl structures) and refined commutator estimates that are uniquely available in the Besov setting. This allows us to obtain endpoint error estimates without the additional fractional derivative loss that arises in the Sobolev calculation.

More importantly, the versatility of our proposed numerical Besov framework extends far beyond the 2D SQG equations. For instance, in the analysis of the 3D Navier–Stokes equations, the same methodology targets the endpoint regularity $u \in L^\infty(0,T;B^2_{\infty,1}(\mathbb{T}^3))$, whereas the Sobolev argument in (Li et al., 2022) uses $u \in L^\infty(0,T;W^{2,12/5}(\mathbb{T}^3))$. This comparison concerns the endpoint structure and the avoidance of a derivative surplus, rather than a set-inclusion improvement, because $B^2_{\infty,1}$ embeds into $W^{2,p}$ for every finite p.

1.5. **Main Numerical Results.** In this section, we present the main theoretical contributions of this paper: the unconditional energy stability and the rigorous error estimates for the proposed LRI (1.1). To isolate the effect of the numerical Besov framework, we first state the benchmark results in the classical Sobolev setting, which naturally exposes the derivative loss phenomenon. Subsequently, we present our sharp results in Besov spaces at the endpoint derivative index.

1. Benchmark: Stability and Error in Sobolev Spaces

Proposition 1.1 (Unconditional Sobolev stability)**.** Consider the SQG equations (SQG) in $\mathbb{T}^2$ with periodic boundary conditions, solved by the semi-implicit low-regularity integrator (LRI) (1.1). Assume that the initial data $\theta_0 \in L^2(\mathbb{T}^2)$. Then, there exists $T > 0$ such that the following statements hold for any $M \in \mathbb{Z}^+$ and $n \le M$, without any restriction on the time step $\tau = \frac{T}{M}$, the viscosity ν, and the dissipative parameter γ:

(i): The L^2 energy dissipates in time:

$$\|\theta^{n+1}\|_{L^2} \le \|\theta^n\|_{L^2}. \tag{1.2}$$

(ii): If we additionally assume $\theta_0 \in H^s(\mathbb{T}^2)$ for $s > 2$, then the H^s norm is uniformly bounded:

$$\sup_n \|\theta^n\|_{H^s} \le 4\|\theta_0\|_{H^s}. \tag{1.3}$$

Proposition 1.2 (Error estimate in Sobolev spaces)**.** Consider the (SQG) equations in a 2D torus $\mathbb{T}^2$ with periodic boundary conditions. Assume that the exact solution satisfies the following regularity:

$$\theta \in C([0,T];L^2(\mathbb{T}^2)) \cap L^\infty(0,T;W^{2,2+\epsilon}(\mathbb{T}^2)), \tag{1.4}$$

where $\epsilon > 0$ is arbitrarily small. Then the numerical solution generated by the LRI (1.1) possesses the following strong error bound:

$$\max_{1\le n\le M} \|\theta(t_n) - \theta^n\|_{L^2} \lesssim \tau,$$

where $M = \frac{T}{\tau}$. For every fixed $\nu_{\max} > 0$, the implied constant is independent of $\nu \in [0,\nu_{\max}]$ and $\gamma \in (0,2]$. In particular, the estimate is uniform in the vanishing-viscosity limit; no uniformity as $\nu \to \infty$ is asserted.

Remark 1.3. It is crucial to note that the stability bound (1.3) and the error estimate in Proposition 1.2 strictly demand the sub-optimal regularity $\theta_0 \in H^s$ $(s > 2)$ or $\theta \in L^\infty(0,T;W^{2,2+\epsilon}(\mathbb{T}^2))$. From the perspective of scaling and Sobolev embeddings, $W^{2,2+\epsilon}(\mathbb{T}^2)$ essentially scales equivalently to $H^{2+\delta}$ for some $\delta > 0$. A similar stringent requirement was adopted by Li, Ma, and Schratz (2022) for the Navier–Stokes equations. This artificial increment in regularity is the unavoidable mathematical consequence of using standard energy estimates to compensate for the derivative loss inherent in the singular fractional convection term.

2. Main Results: Sharp Estimates in the Besov Framework

To fundamentally break the regularity barrier highlighted in Remark 1.3, we now transition to the critically embedded numerical Besov framework. By exploiting delicate div-curl structures and refined product rules in $B^0_{\infty,1}$, we establish the unconditional stability and endpoint error estimates without the additional fractional derivative loss of the Sobolev argument.

Theorem 1.4 (Unconditional Besov stability)**.** Consider the SQG equations (SQG) solved by the LRI (1.1). Assume that the initial data $\theta_0 \in B^1_{\infty,1}(\mathbb{T}^2)$. Then there exists $T > 0$ such that the $B^1_{\infty,1}$ norm is uniformly bounded for any $n \leq M$, unconditionally independent of the time step τ, the viscosity ν, and the dissipative parameter γ:

$$\sup_n \|\theta^n\|_{B^1_{\infty,1}} \leq 4\|\theta_0\|_{B^1_{\infty,1}}. \tag{1.5}$$

Moreover, if $\theta_0 \in B^s_{\infty,1}$ for any $s > 1$, there holds

$$\sup_n \|\theta^n\|_{B^s_{\infty,1}} \leq 4\|\theta_0\|_{B^s_{\infty,1}}. \tag{1.6}$$

Theorem 1.5 (Error estimate in Besov spaces - Endpoint Regularity)**.** Assume that the exact solution to the (SQG) equations satisfies the endpoint Besov regularity:

$$\theta \in C([0,T]; L^2(\mathbb{T}^2)) \cap L^\infty(0,T; B^2_{\infty,1}(\mathbb{T}^2)). \tag{1.7}$$

Then the numerical solution by the LRI (1.1) possesses the following strong error bound:

$$\max_{1\leq n\leq M} \|\theta(t_n) - \theta^n\|_{B^0_{\infty,1}} \lesssim \tau,$$

where, for every fixed $\nu_{\max} > 0$, the implied constant is independent of $\nu \in [0, \nu_{\max}]$ and $\gamma \in (0,2]$. Thus the estimate is uniform as $\nu \to 0$, but not claimed to be uniform for unbounded viscosity.

Remark 1.6 (Comparison and interpretation of the regularity assumptions)**.** The hypotheses in Proposition 1.2 and Theorem 1.5 are conditional regularity assumptions on the exact solution over the interval of comparison. The embedding $W^{2,2+\epsilon}(\mathbb{T}^2) \hookrightarrow W^{1,\infty}(\mathbb{T}^2)$ makes a separate $W^{1,\infty}$ hypothesis in Proposition 1.2 unnecessary. Also, $B^2_{\infty,1}(\mathbb{T}^2) \hookrightarrow W^{2,p}(\mathbb{T}^2)$ for every finite p, so the Besov assumption is not weaker by set inclusion. Its advantage is that it realizes the endpoint derivative index in the Besov error topology and removes the extra ϵ-loss of the Sobolev calculation.

These solution assumptions can be related to the initial data through the well-posedness theory for the SQG equations. Smooth initial data generate local strong solutions with persistence of regularity (Constantin et al., 1994). For $\nu > 0$, global regularity is known in the subcritical regime $\gamma > 1$ (Constantin and Wu, 1999) and in the critical regime $\gamma = 1$ (Kiselev et al., 2007). In contrast, for the inviscid equation $\nu = 0$ and for the supercritical dissipative regime $0 < \gamma < 1$ with general large initial data, global smooth well-posedness remains open. Therefore, a theorem stated solely in terms of θ_0 for all $\nu \geq 0$ and $0 < \gamma \leq 2$ would conceal an unresolved analytical issue. Our error estimates apply on any interval $[0,T]$ on which the indicated exact-solution norm is finite.

1.6. **Organization of the Paper.** The remainder of this paper is organized as follows. In Section 2, we introduce the necessary numerical preliminaries, including the discrete product rules and the essential commutator estimates in Besov spaces. Section 3 is devoted to the unconditional stability and optimal error estimates of the proposed LRI within the classical Sobolev framework. In Section 4, we establish our main theoretical results, detailing the sharp error analysis under the newly introduced numerical Besov framework to overcome the derivative loss. Section 5 provides the full discretization of the LRI utilizing the Fourier spectral method. Finally, in Section 6, we present extensive numerical experiments, that range from rigorous convergence tests to the simulation of complex vortex patch dynamics, to robustly validate our theoretical findings.

2. Numerical Preliminaries

2.1. **Notation.** Throughout this paper, for any two (non-negative) quantities X and Y, we write $X \lesssim Y$ if $X \leq CY$ for some generic constant $C > 0$. Unless stated otherwise, C is independent of the time step τ and $\gamma \in (0, 2]$ and is uniform for ν in a prescribed bounded interval $[0, \nu_{\max}]$; the stability estimates themselves hold for every $\nu \geq 0$. We denote $X \sim Y$ if $X \lesssim Y$ and $Y \lesssim X$. The commutator of two operators is defined as usual by $[A, B] = AB - BA$.

We use the standard convention for the Fourier expansion on the 2D torus $\mathbb{T}^2$:

$$f(x) = \frac{1}{(2\pi)^2} \sum_{k\in\mathbb{Z}^2} \hat{f}(k) e^{ik\cdot x}, \quad \widehat{f}(k) = \int_{\mathbb{T}^2} f(x) e^{-ik\cdot x} \,\mathrm{d}\, x.$$

Based on the Fourier expansion, the equivalent H^s-norm and the homogeneous $\dot{H}^s$-seminorm of a function f are given by

$$\|f\|_{H^s} = \frac{1}{2\pi} \left(\sum_{k\in\mathbb{Z}^2} (1 + |k|^{2s}) |\hat{f}(k)|^2 \right)^{\frac{1}{2}}, \quad \|f\|_{\dot{H}^s} = \frac{1}{2\pi} \left(\sum_{k\in\mathbb{Z}^2} |k|^{2s} |\hat{f}(k)|^2 \right)^{\frac{1}{2}}.$$

To introduce the numerical Besov framework, we recall the Littlewood-Paley dyadic decomposition. Let $\chi : [0, +\infty) \to [0, 1]$ be a smooth, monotonically decreasing cut-off function such that $\chi(r) \equiv 1$ for $0 \leq r \leq \frac{1}{2}$, and $\chi(r) \equiv 0$ for $r \geq 1$. Defining $\varphi(r) = \chi(r) - \chi(2r)$, we have the partition of unity: $\chi(|x|) + \sum_{j\geq1} \varphi(2^{-j}|x|) \equiv 1$ for all $x \in \mathbb{R}^2$. For any distribution f on $\mathbb{T}^2$, the Littlewood-Paley operators are defined as:

$$\begin{cases} \Delta_0 f = \sum_{k\in\mathbb{Z}^2} \hat{f}(k) \chi(|k|) e^{ik\cdot x} = \hat{f}(0), \\ \Delta_j f = \sum_{k\in\mathbb{Z}^2} \hat{f}(k) \varphi(2^{-j}|k|) e^{ik\cdot x}, \quad j \geq 1, \\ S_N f = \sum_{j=0}^{N} \Delta_j f, \quad N \geq 0. \end{cases} \tag{2.1}$$

Throughout this numerical study, we naturally assume that the active scalar θ is of zero mean. Consequently, $\Delta_0 f = 0$ and $f = \sum_{j\geq1} \Delta_j f$.

Let $s \in \mathbb{R}$ and $1 \leq p, r \leq \infty$. The Besov space $B^s_{p,r}(\mathbb{T}^2)$ is defined as the set of distributions satisfying

$$\|f\|_{B^s_{p,r}} = \left\| \left(2^{js} \|\Delta_j f\|_{L^p}\right)_{j\geq1} \right\|_{\ell^r} < \infty. \tag{2.2}$$

2.2. **Essential Estimates for Error Analysis.** The following harmonic analysis tools are vital for establishing our sharp error estimates, which are completely free from derivative loss, for the proposed LRI.

Lemma 2.1 (Bernstein's inequality (Bahouri et al., 2011))**.** Let $1 \leq p \leq q \leq \infty$ and $s \in \mathbb{R}$. Then for any $j \geq 1$, we have

$$C\|\Lambda^s \Delta_j f\|_{L^p} \leq 2^{js} \|\Delta_j f\|_{L^p} \leq C' \|\Lambda^s \Delta_j f\|_{L^p},$$

and

$$\|\Delta_j f\|_{L^q} \lesssim 2^{2j(\frac{1}{p} - \frac{1}{q})} \|\Delta_j f\|_{L^p},$$

where the constants C, C' are strictly independent of j and f.

To carry out the benchmark Sobolev error analysis, we need the Kato-Ponce inequalities:

Lemma 2.2 (Sobolev commutator estimate)**.** Let $s > 0$ and $p \in (1, \infty)$. Suppose $p_1, p_2, p_3, p_4 \in (1, \infty]$ such that $\frac{1}{p} = \frac{1}{p_1} + \frac{1}{p_2} = \frac{1}{p_3} + \frac{1}{p_4}$. Then there exists a constant $C > 0$ such that

$$\|[\Lambda^s, f\cdot]\nabla g\|_{L^p} \leq C\left(\|\Lambda^s f\|_{L^{p_1}}\|\nabla g\|_{L^{p_2}} + \|\nabla f\|_{L^{p_3}}\|\Lambda^s g\|_{L^{p_4}}\right).$$

To bypass the derivative loss inherent in the Sobolev framework, we critically rely on the following commutator and product estimates in the Besov setting.

Lemma 2.3 (Besov commutator estimate)**.** Let $1 \leq p \leq \infty$, $1 \leq r \leq \infty$, $\sigma > -1 - d\min(\frac{1}{p}, \frac{1}{p'})$ and $\operatorname{div} \mathrm{u} = 0$. Define $I_j = [u \cdot \nabla, \Delta_j]f$. Then there exists a constant C such that for $\sigma > 0$, we have

$$\left\|(2^{j\sigma}\|I_j\|_{L^p_x})_j\right\|_{l^r(\mathbb{Z})} \leq C(\|\nabla u\|_{L^\infty}\|f\|_{B^\sigma_{p,r}} + \|\nabla u\|_{B^{\sigma-1}_{p,r}}\|\nabla_x f\|_{L^\infty_x}).$$

Moreover, if $\sigma > 1 + \frac{d}{p}$ or $\sigma = 1 + \frac{d}{p}$, $r = 1$, we have

$$\left\|(2^{j\sigma}\|I_j\|_{L^p_x})_j\right\|_{l^r(\mathbb{Z})} \leq C\|\nabla u\|_{B^{\sigma-1}_{p,r}}\|f\|_{B^\sigma_{p,r}};$$

if $\sigma = 1 + \frac{d}{p}$, $r > 1$, we have

$$\left\|(2^{j\sigma}\|I_j\|_{L^p_x})_j\right\|_{l^r(\mathbb{Z})} \leq C\|\nabla u\|_{B^\sigma_{p,r}}\|f\|_{B^\sigma_{p,r}};$$

if $\sigma < 1 + \frac{d}{p}$, we have

$$\left\|(2^{j\sigma}\|I_j\|_{L^p_x})_j\right\|_{l^r(\mathbb{Z})} \leq C\|\nabla u\|_{B^{\frac{d}{p}}_{p,r}\cap L^\infty}\|f\|_{B^\sigma_{p,r}}.$$

Lemma 2.4. Suppose $\operatorname{div} u = 0$, the following $B^0_{\infty,1}$ estimate holds

$$\|u \cdot \nabla v\|_{B^0_{\infty,1}} \leq C\|u\|_{B^0_{\infty,1}}\|v\|_{B^1_{\infty,1}},$$

for some absolute constant $C > 0$. Furthermore, if in addition both u and v are of zero mean in $\mathbb{T}^2$, then we have:

$$\|f \cdot \nabla g\|_{B^0_{\infty,1}} \lesssim \|f\|_{B^0_{\infty,1}}\|\nabla g\|_{B^0_{\infty,1}}.$$

Finally, since the velocity field u is recovered via the Riesz transform, therefore the boundedness of the Riesz operator is frequently required.

Lemma 2.5 (Boundedness of the Riesz operator $\nabla^\perp\Lambda^{-1}$)**.** Let f be a mean-zero distribution on $\mathbb{T}^2$. The operator $\nabla^\perp\Lambda^{-1}$ is bounded in the following functional spaces:

- For $1 < p < \infty$, $\|\nabla^\perp\Lambda^{-1}f\|_{L^p} \lesssim \|f\|_{L^p}$.
- For $s > 1$, $\|\nabla^\perp\Lambda^{-1}f\|_{L^\infty} \lesssim \|f\|_{H^s}$.
- For the critical Besov space, $\|\nabla^\perp\Lambda^{-1}f\|_{B^0_{\infty,1}} \lesssim \|f\|_{B^0_{\infty,1}}$.

These standard harmonic-analysis estimates follow from Bahouri et al. (2011, Lemma 2.1, Corollary 2.86, and Lemma 2.100) and Li (2019, Theorem 1.1); see also Chapter 2 of Bahouri et al. (2011) for the Fourier-multiplier bounds used in Lemma 2.5.

3. Error Analysis in Sobolev Spaces

This section proves both parts of Proposition 1.1 and then establishes the L^2-error estimate in Proposition 1.2. Subsections 3.1 and 3.2 treat the L^2 and H^s stability estimates, respectively, while Subsection 3.3 contains the error analysis.

3.1. **Unconditional L^2-dissipation.** Recall that θ^{n+1} is generated by the LRI (1.1). Also, it is easy to see that $\nabla \cdot u^n = 0$. We can then test (1.1) with θ^{n+1} and obtain that:

$$\begin{aligned}\|\theta^{n+1}\|_{L^2}^2 =& \left(e^{-\nu\tau\Lambda^\gamma}\theta^n, \theta^{n+1}\right) - \tau\left(e^{-\nu\tau\Lambda^\gamma}u^n \cdot \nabla\theta^{n+1}, \theta^{n+1}\right)\\ \le& \|\theta^{n+1}\|_{L^2}\|\theta^n\|_{L^2}.\end{aligned}$$

We can derive $\|\theta^{n+1}\|_{L^2} \le \|\theta^n\|_{L^2}$ from here and thus prove (1.2).

3.2. **Unconditional H^s-stability.** Throughout this subsection, we assume $s > 2$ as in Proposition 1.1(ii). In this subsection we present the H^s-stability of our LRI (1.1). We first apply Λ^s on both sides of (1.1) and obtain that

$$\Lambda^s\theta^{n+1} + \tau\Lambda^s(e^{-\nu\tau\Lambda^\gamma}u^n \cdot \nabla\theta^{n+1}) = \Lambda^s e^{-\nu\tau\Lambda^\gamma}\theta^n.$$

We then multiply both sides with $\Lambda^s\theta^{n+1}$ and integrate in $\mathbb{T}^2$ to get

$$\begin{aligned}\|\Lambda^s\theta^{n+1}\|_{L^2}^2 =& \left(\Lambda^s e^{-\nu\tau\Lambda^\gamma}\theta^n, \Lambda^s\theta^{n+1}\right) - \tau\left(\Lambda^s(e^{-\nu\tau\Lambda^\gamma}u^n \cdot \nabla\theta^{n+1}), \Lambda^s\theta^{n+1}\right)\\ \le& \|\Lambda^s\theta^{n+1}\|_{L^2}\|\Lambda^s\theta^n\|_{L^2} - \tau\left(e^{-\nu\tau\Lambda^\gamma}u^n \cdot \nabla\Lambda^s\theta^{n+1}, \Lambda^s\theta^{n+1}\right)\\ &- \tau\left([\Lambda^s, e^{-\nu\tau\Lambda^\gamma}u^n \cdot \nabla]\theta^{n+1}, \Lambda^s\theta^{n+1}\right)\\ \le& \|\Lambda^s\theta^{n+1}\|_{L^2}\|\Lambda^s\theta^n\|_{L^2} + C\tau\|\nabla e^{-\nu\tau\Lambda^\gamma}u^n\|_{L^\infty}\|\theta^{n+1}\|_{H^s}\|\Lambda^s\theta^{n+1}\|_{L^2}\\ &+ C\tau\|\nabla e^{-\nu\tau\Lambda^\gamma}u^n\|_{H^{s-1}}\|\nabla\theta^{n+1}\|_{L^\infty}\|\Lambda^s\theta^{n+1}\|_{L^2}\\ \le& \|\Lambda^s\theta^{n+1}\|_{L^2}\|\Lambda^s\theta^n\|_{L^2} + C\tau\|u^n\|_{H^s}\|\theta^{n+1}\|_{H^s}\|\Lambda^s\theta^{n+1}\|_{L^2},\end{aligned}$$

where the last two inequalities follow from Lemma 2.3 by taking $p = r = 2$ and identifying $B^s_{2,2} \sim H^s$. By Lemma 2.5 we have

$$\|\theta^{n+1}\|_{H^s}^2 \le \|\theta^n\|_{H^s}^2 + C\tau\|\theta^n\|_{H^s}\|\theta^{n+1}\|_{H^s}^2,$$

for some absolute constant $C > 0$. Without loss of generality, we can assume $T = \frac{1}{4C\|\theta_0\|_{H^s}}$ and $\tau = \frac{T}{M}$ from the local well-posedness theory and $\|\theta^n\|_{H^s} \le 4\|\theta_0\|_{H^s}$ as an induction hypothesis. We thus get that

$$\|\theta^{n+1}\|_{H^s}^2 \le \|\theta^n\|_{H^s}^2 + \frac{1}{M}\|\theta^{n+1}\|_{H^s}^2,$$

which implies that

$$\|\theta^{n+1}\|_{H^s}^2 \le (1+h)\|\theta^n\|_{H^s}^2,$$

where $h := \frac{1}{M-1}$. Iterating the inequality above, we have

$$\begin{aligned}\|\theta^{n+1}\|_{H^s}^2 &\le (1+h)^{M+1}\|\theta_0\|_{H^s}^2\\ &\le (1+h)^{\frac{1}{h}+2}\|\theta_0\|_{H^s}^2\\ &\le 16\|\theta_0\|_{H^s}^2.\end{aligned}$$

This then proves (1.3) and thus shows Proposition 1.1.

3.3. **L^2 error estimate.** It is known that the exact solution of (SQG) can be written in the following Duhamel's formula for any $s \in [t_n, t_{n+1}]$:

$$\theta(s) = e^{-\nu(s-t_n)\Lambda^\gamma}\theta(t_n) - \int_{t_n}^{s} e^{-\nu(s-\sigma)\Lambda^\gamma}\left(\nabla^\perp\Lambda^{-1}\theta \cdot \nabla\theta\right)(\sigma)\ \mathrm{d}\sigma\,. \tag{3.1}$$

In particular, we have

$$\theta(t_{n+1}) = e^{-\nu\tau\Lambda^\gamma}\theta(t_n) - \int_{t_n}^{t_{n+1}} e^{-\nu(t_{n+1}-s)\Lambda^\gamma}\left(\nabla^\perp\Lambda^{-1}\theta \cdot \nabla\theta\right)(s)\,\mathrm{d}s\,. \tag{3.2}$$

Note that for $s \in [t_n, t_{n+1}]$, we can approximate $\theta(s)$ by $e^{-\nu(s-t_n)\Lambda^\gamma}\theta(t_n)$ as in (3.1):

$$\begin{aligned}
&\int_{t_n}^{t_{n+1}} e^{-\nu(t_{n+1}-s)\Lambda^\gamma} \left(\nabla^\perp\Lambda^{-1}\theta\cdot\nabla\theta\right)(s)\,\mathrm{ds} \\
=&\int_{t_n}^{t_{n+1}} e^{-\nu(t_{n+1}-s)\Lambda^\gamma} \left(e^{-\nu(s-t_n)\Lambda^\gamma}\nabla^\perp\Lambda^{-1}\theta(t_n)\cdot\nabla e^{-\nu(s-t_n)\Lambda^\gamma}\theta(t_n)\right)\mathrm{ds}+R_{n,1},
\end{aligned}$$

where the remaining term is the following:

$$\begin{aligned}
R_{n,1} =& \int_{t_n}^{t_{n+1}} e^{-\nu(t_{n+1}-s)\Lambda^\gamma} \left(\nabla^\perp\Lambda^{-1}\theta\cdot\nabla\theta\right)(s)\,\mathrm{ds} \\
&-\int_{t_n}^{t_{n+1}} e^{-\nu(t_{n+1}-s)\Lambda^\gamma} \left(e^{-\nu(s-t_n)\Lambda^\gamma}\nabla^\perp\Lambda^{-1}\theta(t_n)\cdot\nabla e^{-\nu(s-t_n)\Lambda^\gamma}\theta(t_n)\right)\mathrm{ds} \\
=&\int_{t_n}^{t_{n+1}} e^{-\nu(t_{n+1}-s)\Lambda^\gamma} \left(\nabla^\perp\Lambda^{-1}(\theta(s)-e^{-\nu(s-t_n)\Lambda^\gamma}\theta(t_n))\cdot\nabla\theta(s)\right)\mathrm{ds} \\
&+\int_{t_n}^{t_{n+1}} e^{-\nu(t_{n+1}-s)\Lambda^\gamma} \left(\nabla^\perp\Lambda^{-1}e^{-\nu(s-t_n)\Lambda^\gamma}\theta(t_n)\cdot\nabla(\theta(s)-e^{-\nu(s-t_n)\Lambda^\gamma}\theta(t_n))\right)\mathrm{ds}\,.
\end{aligned} \tag{3.3}$$

Therefore we can rewrite (3.2) as below

$$\theta(t_{n+1}) = e^{-\nu\tau\Lambda^\gamma}\theta(t_n) - \int_{t_n}^{t_{n+1}} g(s)\,\mathrm{ds} - R_{n,1}, \tag{3.4}$$

where $g(s) = e^{-\nu(t_{n+1}-s)\Lambda^\gamma}(\nabla^\perp\Lambda^{-1}v(s)\cdot\nabla v(s))$, with $v(s) = e^{-\nu(s-t_n)\Lambda^\gamma}\theta(t_n)$.

Besides, we can further approximate $\int_{t_n}^{t_{n+1}} g(s)\ \mathrm{ds}$ by observing that

$$g(s) = g(t_{n+1}) - \int_s^{t_{n+1}} \partial_\sigma g(\sigma)\,\mathrm{d}\sigma\,.$$

Therefore (3.4) can be reorganized as

$$\theta(t_{n+1}) = e^{-\nu\tau\Lambda^\gamma}\theta(t_n) - \int_{t_n}^{t_{n+1}} g(t_{n+1})\,\mathrm{ds} - R_{n,1} - R_{n,2},$$

where $R_{n,2} = \int_{t_n}^{t_{n+1}} g(s) - g(t_{n+1})\,\mathrm{ds}$. Writing $g(t_{n+1})$ out explicitly, we have

$$\theta(t_{n+1}) = e^{-\nu\tau\Lambda^\gamma}\theta(t_n) - \tau\left(\nabla^\perp\Lambda^{-1}e^{-\nu\tau\Lambda^\gamma}\theta(t_n)\cdot\nabla e^{-\nu\tau\Lambda^\gamma}\theta(t_n)\right) - R_{n,1} - R_{n,2}. \tag{3.5}$$

From (3.5), we can further derive that

$$\theta(t_{n+1}) = e^{-\nu\tau\Lambda^\gamma}\theta(t_n) - \tau\left(\nabla^\perp\Lambda^{-1}e^{-\nu\tau\Lambda^\gamma}\theta(t_n)\cdot\nabla\theta(t_{n+1})\right) - R_{n,1} - R_{n,2} - R_{n,3}, \tag{3.6}$$

where

$$\begin{aligned}
R_{n,3} &= \tau\left(\nabla^\perp\Lambda^{-1}e^{-\nu\tau\Lambda^\gamma}\theta(t_n)\cdot\nabla(e^{-\nu\tau\Lambda^\gamma}\theta(t_n)-\theta(t_{n+1}))\right) \\
&= \tau\left(\nabla^\perp\Lambda^{-1}e^{-\nu\tau\Lambda^\gamma}\theta(t_n)\cdot\nabla\int_{t_n}^{t_{n+1}} e^{-\nu(t_{n+1}-s)\Lambda^\gamma}(\nabla^\perp\Lambda^{-1}\theta(s)\cdot\nabla\theta(s))\,\mathrm{ds}\right).
\end{aligned} \tag{3.7}$$

Next, we estimate the terms $R_{n,1}$, $R_{n,2}$ and $R_{n,3}$. To start with, it is clear from (3.3) and (3.1) that

$$\begin{aligned}\|R_{n,1}\|_{L^2} \leq &\int_{t_n}^{t_{n+1}} \left\|\nabla^\perp\Lambda^{-1}(\theta(s)-e^{-\nu(s-t_n)\Lambda^\gamma}\theta(t_n))\cdot\nabla\theta(s)\right\|_{L^2}\mathrm{ds}\\ &+\int_{t_n}^{t_{n+1}}\left\|\nabla^\perp\Lambda^{-1}e^{-\nu(s-t_n)\Lambda^\gamma}\theta(t_n)\cdot\nabla(\theta(s)-e^{-\nu(s-t_n)\Lambda^\gamma}\theta(t_n))\right\|_{L^2}\mathrm{ds}\\ \leq&\tau\sup_{s\in[t_n,t_{n+1}]}\Big\{\|\nabla^\perp\Lambda^{-1}(\theta(s)-e^{-\nu(s-t_n)\Lambda^\gamma}\theta(t_n))\|_{L^{p_1}}\|\nabla\theta(s)\|_{L^{q_1}}\\ &+\|\nabla^\perp\Lambda^{-1}\theta(t_n)\|_{L^{p_2}}\|\nabla(\theta(s)-e^{-\nu(s-t_n)\Lambda^\gamma}\theta(t_n))\|_{L^{q_2}}\Big\},\end{aligned}\tag{3.8}$$

where $p_i,q_i\in[2,\infty]$ are arbitrary so long as $\frac{1}{p_i}+\frac{1}{q_i}=\frac{1}{2}$. Note that here $\nabla^\perp\Lambda^{-1}$ is a Riesz operator and θ is mean-zero. By Lemma 2.5 and (3.8), we have

$$\begin{aligned}\|R_{n,1}\|_{L^2}\lesssim&\tau^2(\|\nabla\theta\|_{L_t^\infty L^4}\|\nabla^\perp\Lambda^{-1}\theta\cdot\nabla\theta\|_{L_t^\infty L^4}+\|\nabla^\perp\Lambda^{-1}\theta\|_{L_t^\infty L^\infty}\|\nabla(\nabla^\perp\Lambda^{-1}\theta\cdot\nabla\theta)\|_{L_t^\infty L^2})\\ \lesssim&\tau^2(\|\theta\|_{L_t^\infty H^2}\|\theta\|^2_{L_t^\infty W^{1,4}}+\|\theta\|_{L_t^\infty L^2}\|\theta\|^2_{L_t^\infty H^2})\\ \lesssim&\tau^2\|\theta\|^3_{L_t^\infty H^2}.\end{aligned}\tag{3.9}$$

To estimate $R_{n,2}$ we first observe that

$$\begin{aligned}\partial_\sigma g(\sigma)=&e^{-\nu(t_{n+1}-\sigma)\Lambda^\gamma}\nu\Lambda^\gamma(\nabla^\perp\Lambda^{-1}v(\sigma)\cdot\nabla v(\sigma))\\ &-e^{-\nu(t_{n+1}-\sigma)\Lambda^\gamma}\Big(\nu\Lambda^\gamma\nabla^\perp\Lambda^{-1}v(\sigma)\cdot\nabla v(\sigma)\Big)\\ &-e^{-\nu(t_{n+1}-\sigma)\Lambda^\gamma}\Big(\nabla^\perp\Lambda^{-1}v(\sigma)\cdot\nu\Lambda^\gamma\nabla v(\sigma)\Big)\\ =&-\nu e^{-\nu(t_{n+1}-\sigma)\Lambda^\gamma}\Big(\Lambda^\gamma\nabla^\perp\Lambda^{-1}v(\sigma)\cdot\nabla v(\sigma)\Big)\\ &+\nu e^{-\nu(t_{n+1}-\sigma)\Lambda^\gamma}[\Lambda^\gamma,\nabla^\perp\Lambda^{-1}v(\sigma)\cdot\nabla]v(\sigma).\end{aligned}\tag{3.10}$$

Then we have by (3.10)

$$\begin{aligned}\|R_{n,2}\|_{L^2}\lesssim&\tau\sup_{s\in[t_n,t_{n+1}]}\|g(s)-g(t_{n+1})\|_{L^2}\\ \lesssim&\tau^2\sup_{s\in[t_n,t_{n+1}],\sigma\in[s,t_{n+1}]}\|\partial_\sigma g\|_{L^2}\\ \lesssim&\nu\tau^2\|\Big[\Lambda^\gamma,\nabla^\perp\Lambda^{-1}v\cdot\nabla\Big]v\|_{L_t^\infty L^2}+\nu\tau^2\|\Lambda^\gamma\nabla^\perp\Lambda^{-1}v\cdot\nabla v\|_{L_t^\infty L^2}\\ :=&\nu\tau^2I_1+\nu\tau^2I_2.\end{aligned}$$

To estimate I_2, it is clear by Hölder's inequality and Lemma 2.5 that

$$I_2=\|\Lambda^\gamma\nabla^\perp\Lambda^{-1}v\cdot\nabla v\|_{L_t^\infty L^2}\lesssim\|\Lambda^\gamma v\|_{L_t^\infty L^p}\|\nabla v\|_{L_t^\infty L^q},$$

where $\frac{1}{p}+\frac{1}{q}=\frac{1}{2}$. Since $0<\gamma\leq 2$, we then take $p=2+\epsilon$ where $\epsilon>0$ is arbitrarily small. Then I_2 can be estimated after applying the $H^1(\mathbb{T}^2)\hookrightarrow L^q(\mathbb{T}^2)$ Sobolev embedding:

$$I_2\lesssim\|\Lambda^\gamma v\|_{L_t^\infty L^{2+\epsilon}}\|v\|_{L_t^\infty H^2}\lesssim\|v\|^2_{L_t^\infty W^{2,2+\epsilon}}\lesssim\|\theta\|^2_{L_t^\infty W^{2,2+\epsilon}}.\tag{3.11}$$

It is worth emphasizing that the estimate (3.11) is independent of the choice of ν and γ. Note that here the semigroup $e^{-\nu(s-t_n)\Lambda^\gamma}$ is bounded independently of ν and γ in $L^{2+\epsilon}$. Similarly we can estimate I_1 by adopting the Sobolev commutator estimate Lemma 2.2:

$$\begin{aligned}I_1=&\|\Big[\Lambda^\gamma,\nabla^\perp\Lambda^{-1}v\cdot\nabla\Big]v\|_{L_t^\infty L^2}\\ \lesssim&\|\Lambda^\gamma\nabla^\perp\Lambda^{-1}v\|_{L_t^\infty L^{p_3}}\|\nabla v\|_{L_t^\infty L^{q_3}}+\|\Lambda^{\gamma-1}\nabla v\|_{L_t^\infty L^{p_4}}\|\nabla\nabla^\perp\Lambda^{-1}v\|_{L_t^\infty L^{q_4}},\end{aligned}$$

where again $p_i, q_i \in [2,\infty)$ and $\frac{1}{p_i}+\frac{1}{q_i}=\frac{1}{2}$. Then by Lemma 2.5 we have

$$I_1 \lesssim \|\Lambda^\gamma v\|_{L_t^\infty L^{2+\epsilon}} \|v\|_{L_t^\infty H^2} \lesssim \|\theta\|^2_{L_t^\infty W^{2,2+\epsilon}}. \tag{3.12}$$

Combining (3.11)-(3.12), we can conclude

$$\|R_{n,2}\|_{L^2} \lesssim \nu\tau^2 \|\theta\|^2_{L_t^\infty W^{2,2+\epsilon}}. \tag{3.13}$$

Moreover, we can estimate $R_{n,3}$ from (3.7) as follows:

$$\|R_{n,3}\|_{L^2} \lesssim \tau^2 \|\nabla^\perp \Lambda^{-1}\theta\|_{L_t^\infty L^\infty} \|\nabla(\nabla^\perp\Lambda^{-1}\theta\cdot\nabla\theta)\|_{L_t^\infty L^2} \lesssim \tau^2\|\theta\|^3_{L_t^\infty H^2}. \tag{3.14}$$

Now we let $\mathcal{E}^{n+1} = \theta^{n+1} - \theta(t_{n+1})$ be the error. Then we can derive from (3.6) that

$$\begin{aligned} \mathcal{E}^{n+1} + \tau\left(e^{-\nu\tau\Lambda^\gamma}\nabla^\perp\Lambda^{-1}\theta^n\cdot\nabla\mathcal{E}^{n+1}\right) =& e^{-\nu\tau\Lambda^\gamma}\mathcal{E}^n - \tau\left(e^{-\nu\tau\Lambda^\gamma}\nabla^\perp\Lambda^{-1}\mathcal{E}^n\cdot\nabla\theta(t_{n+1})\right) \\ &+ R_{n,1}+R_{n,2}+R_{n,3}. \end{aligned} \tag{3.15}$$

We take the L^2-inner product between (3.15) and $\mathcal{E}^{n+1}$. Note that $\operatorname{div}\nabla^\perp\Lambda^{-1}\theta^n=0$, we therefore obtain that

$$\begin{aligned} \|\mathcal{E}^{n+1}\|^2_{L^2} =& \left(e^{-\nu\tau\Lambda^\gamma}\mathcal{E}^n, \mathcal{E}^{n+1}\right) - \tau\left(e^{-\nu\tau\Lambda^\gamma}\nabla^\perp\Lambda^{-1}\mathcal{E}^n\cdot\nabla\theta(t_{n+1}), \mathcal{E}^{n+1}\right) \\ &+ \left(R_{n,1}+R_{n,2}+R_{n,3}, \mathcal{E}^{n+1}\right) \\ \le& \frac{1}{2}\|\mathcal{E}^n\|^2_{L^2} + \frac{1}{2}\|\mathcal{E}^{n+1}\|^2_{L^2} + C\tau\|\nabla\theta(t_{n+1})\|_{L^\infty}\|\mathcal{E}^n\|_{L^2}\|\mathcal{E}^{n+1}\|_{L^2} + C\tau^2\|\mathcal{E}^{n+1}\|_{L^2} \\ &+ C\nu\tau^2\|\mathcal{E}^{n+1}\|_{L^2} \\ \le& \frac{1}{2}\|\mathcal{E}^n\|^2_{L^2} + \frac{1}{2}\|\mathcal{E}^{n+1}\|^2_{L^2} + C\tau\|\mathcal{E}^n\|^2_{L^2} + C\tau\|\mathcal{E}^{n+1}\|^2_{L^2} + C\tau^3 + C\nu^2\tau^3, \end{aligned} \tag{3.16}$$

by applying (3.9), (3.13) and (3.14). The factor $\|\nabla\theta(t_{n+1})\|_{L^\infty}$ is controlled by $\|\theta\|_{W^{2,2+\epsilon}}$ through the embedding $W^{2,2+\epsilon}(\mathbb{T}^2) \hookrightarrow W^{1,\infty}(\mathbb{T}^2)$, so no separate $W^{1,\infty}$ assumption is needed. Then we derive from (3.16) that

$$\|\mathcal{E}^{n+1}\|^2_{L^2} \le \frac{1+C^*\tau}{1-C^*\tau}\|\mathcal{E}^n\|^2_{L^2} + \frac{C^*(1+\nu^2)\tau^3}{1-C^*\tau},$$

for a constant C^* depending on the displayed exact-solution norms. On each interval $0\le\nu\le\nu_{\max}$, the factor $1+\nu^2$ is bounded independently of ν. By the discrete Grönwall's inequality (cf. Cheng et al., 2024a) we arrive at

$$\sup_n \|\mathcal{E}^n\|_{L^2} \lesssim \tau,$$

where we need

$$\theta \in C([0,T]; L^2(\mathbb{T}^2)) \cap L^\infty(0,T; W^{2,2+\epsilon}(\mathbb{T}^2)).$$

This completes the proof of Proposition 1.2.

4. Sharp Error Analysis in Besov Spaces

In this section we prove Theorem 1.5 by performing the $B^0_{\infty,1}$-error estimates. We first show the stability result in Theorem 1.4:

4.1. **Unconditional $B^1_{\infty,1}$ stability.** Recall our LRI (1.1):

$$\theta^{n+1} + \tau(e^{-\nu\tau\Lambda^\gamma} u^n \cdot \nabla\theta^{n+1}) = e^{-\nu\tau\Lambda^\gamma}\theta^n. \tag{4.1}$$

Applying the Littlewood-Paley frequency projection on both sides of (4.1) we can derive that

$$\begin{aligned}\Delta_j\theta^{n+1} &= \Delta_j e^{-\nu\tau\Lambda^\gamma}\theta^n - \tau\Delta_j\left(e^{-\nu\tau\Lambda^\gamma}\nabla^\perp\Lambda^{-1}\theta^n\cdot\nabla\theta^{n+1}\right)\\ &= \Delta_j e^{-\nu\tau\Lambda^\gamma}\theta^n - \tau e^{-\nu\tau\Lambda^\gamma}\nabla^\perp\Lambda^{-1}\theta^n\cdot\nabla\Delta_j\theta^{n+1} - \tau\left(\left[\Delta_j, e^{-\nu\tau\Lambda^\gamma}\nabla^\perp\Lambda^{-1}\theta^n\cdot\nabla\right]\theta^{n+1}\right).\end{aligned} \tag{4.2}$$

Taking $\mathrm{sgn}(\Delta_j\theta^{n+1})|\Delta_j\theta^{n+1}|^{p-1}$ as a test function of (4.2), we can then obtain the following energy estimate:

$$2^j\|\Delta_j\theta^{n+1}\|_{L^p} \le 2^j\|\Delta_j\theta^n\|_{L^p} + 2^j\tau\|\left[e^{-\nu\tau\Lambda^\gamma}\nabla^\perp\Lambda^{-1}\theta^n\cdot\nabla, \Delta_j\right]\theta^{n+1}\|_{L^p}.$$

Taking $p=\infty$ and summing the series in j, we can get

$$\|\theta^{n+1}\|_{B^1_{\infty,1}} \le \|\theta^n\|_{B^1_{\infty,1}} + C\tau\|\theta^n\|_{B^1_{\infty,1}}\|\theta^{n+1}\|_{B^1_{\infty,1}},$$

where $C>0$ is an absolute constant. With no loss we can again assume $T = \frac{1}{4C\|\theta_0\|_{B^1_{\infty,1}}}$ and $\tau = \frac{T}{M}$. Similar to Proposition 1.1 we can further assume $\|\theta^n\|_{B^1_{\infty,1}} \le 4\|\theta_0\|_{B^1_{\infty,1}}$ as an induction hypothesis. It then follows that

$$\|\theta^{n+1}\|_{B^1_{\infty,1}} \le (1+h)\|\theta^n\|_{B^1_{\infty,1}},$$

where $h := \frac{1}{M-1}$. Iterating the inequality above, we get

$$\|\theta^{n+1}\|_{B^1_{\infty,1}} \le 4\|\theta_0\|_{B^1_{\infty,1}}.$$

Invoking the Besov commutator estimate (Lemma 2.3), we deduce that

$$\sum_{j=0}^\infty 2^{sj}\tau\|\left[e^{-\nu\tau\Lambda^\gamma}\nabla^\perp\Lambda^{-1}\theta^n\cdot\nabla,\Delta_j\right]\theta^{n+1}\|_{L^\infty} \le \tau(\|\theta^n\|_{B^1_{\infty,1}}\|\theta^{n+1}\|_{B^s_{\infty,1}} + \|\theta^n\|_{B^s_{\infty,1}}\|\theta^{n+1}\|_{B^1_{\infty,1}}),$$

which implies that

$$\begin{aligned}\|\theta^{n+1}\|_{B^s_{\infty,1}} &\le \|\theta^n\|_{B^s_{\infty,1}} + C\tau(\|\theta^n\|_{B^1_{\infty,1}}\|\theta^{n+1}\|_{B^s_{\infty,1}} + \|\theta^n\|_{B^s_{\infty,1}}\|\theta^{n+1}\|_{B^1_{\infty,1}})\\ &\le \|\theta^n\|_{B^s_{\infty,1}} + 4C\tau\|\theta_0\|_{B^1_{\infty,1}}(\|\theta^{n+1}\|_{B^s_{\infty,1}} + \|\theta^n\|_{B^s_{\infty,1}})\\ &\le \|\theta^n\|_{B^s_{\infty,1}} + \frac{1}{M}(\|\theta^{n+1}\|_{B^s_{\infty,1}} + \|\theta^n\|_{B^s_{\infty,1}}).\end{aligned}$$

Then we deduce that

$$\|\theta^{n+1}\|_{B^s_{\infty,1}} \le (1+2h)\|\theta^n\|_{B^s_{\infty,1}},$$

Iterating the inequality above, we have

$$\|\theta^{n+1}\|_{B^s_{\infty,1}} \le 4\|\theta_0\|_{B^s_{\infty,1}}.$$

This completes the proof of Theorem 1.4.

4.2. $B^0_{\infty,1}$**-error estimate.** Similar to Section 3 we write the exact solution of (SQG) in the following Duhamel's formula for any $s \in [t_n, t_{n+1}]$:

$$\theta(s) = e^{-\nu(s-t_n)\Lambda^\gamma}\theta(t_n) - \int_{t_n}^{s} e^{-\nu(s-\sigma)\Lambda^\gamma}\left(\nabla^\perp\Lambda^{-1}\theta\cdot\nabla\theta\right)(\sigma)\,\mathrm{d}\sigma\,. \tag{4.3}$$

In particular, we again have

$$\theta(t_{n+1}) = e^{-\nu\tau\Lambda^\gamma}\theta(t_n) - \int_{t_n}^{t_{n+1}} e^{-\nu(t_{n+1}-s)\Lambda^\gamma}\left(\nabla^\perp\Lambda^{-1}\theta\cdot\nabla\theta\right)(s)\,\mathrm{d}s\,. \tag{4.4}$$

After applying the Littlewood-Paley frequency projection Δ_j, we have the following approximation for $s \in [t_n, t_{n+1}]$:

$$\begin{aligned}&\int_{t_n}^{t_{n+1}} \Delta_j e^{-\nu(t_{n+1}-s)\Lambda^\gamma}\left(\nabla^\perp\Lambda^{-1}\theta\cdot\nabla\theta\right)(s)\,\mathrm{d}s\\ &=\int_{t_n}^{t_{n+1}} \Delta_j e^{-\nu(t_{n+1}-s)\Lambda^\gamma}\left(e^{-\nu(s-t_n)\Lambda^\gamma}\nabla^\perp\Lambda^{-1}\theta(t_n)\cdot\nabla e^{-\nu(s-t_n)\Lambda^\gamma}\theta(t_n)\right)\mathrm{d}s + B_{n,1},\end{aligned} \tag{4.5}$$

where the remaining term is the following:

$$\begin{aligned}B_{n,1} =& \int_{t_n}^{t_{n+1}} \Delta_j e^{-\nu(t_{n+1}-s)\Lambda^\gamma}\left(\nabla^\perp\Lambda^{-1}\theta\cdot\nabla\theta\right)(s)\,\mathrm{d}s\\ &- \int_{t_n}^{t_{n+1}} \Delta_j e^{-\nu(t_{n+1}-s)\Lambda^\gamma}\left(e^{-\nu(s-t_n)\Lambda^\gamma}\nabla^\perp\Lambda^{-1}\theta(t_n)\cdot\nabla e^{-\nu(s-t_n)\Lambda^\gamma}\theta(t_n)\right)\mathrm{d}s\\ =& \int_{t_n}^{t_{n+1}} \Delta_j e^{-\nu(t_{n+1}-s)\Lambda^\gamma}\left(\nabla^\perp\Lambda^{-1}(\theta(s) - e^{-\nu(s-t_n)\Lambda^\gamma}\theta(t_n))\cdot\nabla\theta(s)\right)\mathrm{d}s\\ &+ \int_{t_n}^{t_{n+1}} \Delta_j e^{-\nu(t_{n+1}-s)\Lambda^\gamma}\left(\nabla^\perp\Lambda^{-1}e^{-\nu(s-t_n)\Lambda^\gamma}\theta(t_n)\cdot\nabla(\theta(s) - e^{-\nu(s-t_n)\Lambda^\gamma}\theta(t_n))\right)\mathrm{d}s\,.\end{aligned} \tag{4.6}$$

Combining (4.4) and (4.5), we infer that

$$\begin{aligned}&\Delta_j\theta(t_{n+1})\\ =&\Delta_j e^{-\nu\tau\Lambda^\gamma}\theta(t_n) - \int_{t_n}^{t_{n+1}} \Delta_j e^{-\nu(t_{n+1}-s)\Lambda^\gamma}\left(e^{-\nu(s-t_n)\Lambda^\gamma}\nabla^\perp\Lambda^{-1}\theta(t_n)\cdot\nabla e^{-\nu(s-t_n)\Lambda^\gamma}\theta(t_n)\right)\mathrm{d}s - B_{n,1}\\ =&\Delta_j e^{-\nu\tau\Lambda^\gamma}\theta(t_n) - \int_{t_n}^{t_{n+1}} h(s)\,\mathrm{d}s - B_{n,1},\end{aligned} \tag{4.7}$$

where $h(s) = \Delta_j e^{-\nu(t_{n+1}-s)\Lambda^\gamma}(\nabla^\perp\Lambda^{-1}v(s)\cdot\nabla v(s))$, with $v(s) = e^{-\nu(s-t_n)\Lambda^\gamma}\theta(t_n)$. Besides, we can further approximate $\int_{t_n}^{t_{n+1}} h(s)\ \mathrm{d}s$ by observing that

$$h(s) = h(t_{n+1}) - \int_s^{t_{n+1}} \partial_\sigma h(\sigma)\,\mathrm{d}\sigma\,.$$

Therefore (4.7) can be reorganized as

$$\Delta_j\theta(t_{n+1}) = \Delta_j e^{-\nu\tau\Lambda^\gamma}\theta(t_n) - \int_{t_n}^{t_{n+1}} h(t_{n+1})\,\mathrm{d}s - B_{n,1} - B_{n,2},$$

where $B_{n,2} = \int_{t_n}^{t_{n+1}} h(s) - h(t_{n+1})\,\mathrm{d}s$. Writing $h(t_{n+1})$ out explicitly we have

$$\Delta_j\theta(t_{n+1}) = \Delta_j e^{-\nu\tau\Lambda^\gamma}\theta(t_n) - \tau\Delta_j\left(\nabla^\perp\Lambda^{-1}e^{-\nu\tau\Lambda^\gamma}\theta(t_n)\cdot\nabla e^{-\nu\tau\Lambda^\gamma}\theta(t_n)\right) - B_{n,1} - B_{n,2}. \tag{4.8}$$

From (4.8) we can further derive that

$$\Delta_j\theta(t_{n+1}) = \Delta_j e^{-\nu\tau\Lambda^\gamma}\theta(t_n) - \tau\Delta_j\left(\nabla^\perp\Lambda^{-1}e^{-\nu\tau\Lambda^\gamma}\theta(t_n)\cdot\nabla\theta(t_{n+1})\right) - B_{n,1} - B_{n,2} - B_{n,3}, \tag{4.9}$$

where

$$\begin{aligned} B_{n,3} &= \tau\Delta_j\left(\nabla^\perp\Lambda^{-1}e^{-\nu\tau\Lambda^\gamma}\theta(t_n)\cdot\nabla(e^{-\nu\tau\Lambda^\gamma}\theta(t_n) - \theta(t_{n+1}))\right) \\ &= \tau\Delta_j\left(\nabla^\perp\Lambda^{-1}e^{-\nu\tau\Lambda^\gamma}\theta(t_n)\cdot\nabla\int_{t_n}^{t_{n+1}} e^{-\nu(t_{n+1}-s)\Lambda^\gamma}(\nabla^\perp\Lambda^{-1}\theta(s)\cdot\nabla\theta(s))\,\mathrm{ds}\right). \end{aligned} \tag{4.10}$$

Next, we estimate the terms $B_{n,1}$, $B_{n,2}$ and $B_{n,3}$. Firstly, it is clear from (4.3) and (4.6) that

$$\begin{aligned} &B_{n,1} \\ =&\int_{t_n}^{t_{n+1}} \Delta_j e^{-\nu(t_{n+1}-s)\Lambda^\gamma}\left(\nabla^\perp\Lambda^{-1}\int_{t_n}^{s} e^{-\nu(s-\sigma)\Lambda^\gamma}(\nabla^\perp\Lambda^{-1}\theta\cdot\nabla\theta)(\sigma)\ \mathrm{d}\sigma\cdot\nabla\theta(s)\right)\ \mathrm{ds} \\ &+\int_{t_n}^{t_{n+1}} \Delta_j e^{-\nu(t_{n+1}-s)\Lambda^\gamma}\left(e^{-\nu(s-t_n)\Lambda^\gamma}\nabla^\perp\Lambda^{-1}\theta(t_n)\cdot\nabla\int_{t_n}^{s} e^{-\nu(s-\sigma)\Lambda^\gamma}(\nabla^\perp\Lambda^{-1}\theta\cdot\nabla\theta)(\sigma)\ \mathrm{d}\sigma\right)\ \mathrm{ds} \\ \coloneqq& B_{n,1,I} + B_{n,1,II}. \end{aligned} \tag{4.11}$$

Therefore we consider $B_{n,1,I}$ and $B_{n,1,II}$ respectively.

$$B_{n,1,I} = \int_{t_n}^{t_{n+1}} \Delta_j e^{-\nu(t_{n+1}-s)\Lambda^\gamma}\left(\nabla^\perp\Lambda^{-1}V(s)\cdot\nabla\theta(s)\right)\ \mathrm{ds},$$

where we define

$$V(s) \coloneqq \int_{t_n}^{s} e^{-\nu(s-\sigma)\Lambda^\gamma}(\nabla^\perp\Lambda^{-1}\theta\cdot\nabla\theta)(\sigma)\ \mathrm{d}\sigma\,. \tag{4.12}$$

Noting that $\operatorname{div}\nabla^\perp\Lambda^{-1}\theta = 0$ then by Lemma 2.4 we have

$$\|\nabla^\perp\Lambda^{-1}\theta\cdot\nabla\theta\|_{L_t^\infty B^0_{\infty,1}} \lesssim \|\nabla^\perp\Lambda^{-1}\theta\|_{L_t^\infty B^0_{\infty,1}}\|\theta\|_{L_t^\infty B^1_{\infty,1}}.$$

We observe that by Lemma 2.5, $V(s)$ can be bounded further by

$$\|V(s)\|_{B^0_{\infty,1}} \lesssim \tau\|\nabla^\perp\Lambda^{-1}\theta\|_{L_t^\infty B^0_{\infty,1}}\|\theta\|_{L_t^\infty B^1_{\infty,1}} \lesssim \tau\|\theta\|_{L_t^\infty B^0_{\infty,1}}\|\theta\|_{L_t^\infty B^1_{\infty,1}}. \tag{4.13}$$

Moreover by the div-curl structure noting $\operatorname{div}\nabla^\perp\Lambda^{-1}V = 0$ we have (again by Lemma 2.4)

$$\begin{aligned} \sum_j \|B_{n,1,I}\|_{L^\infty} \lesssim&\tau\|\nabla^\perp\Lambda^{-1}V\|_{L_t^\infty B^0_{\infty,1}}\|\theta\|_{L_t^\infty B^1_{\infty,1}} \\ \lesssim&\tau^2\|\theta\|_{L_t^\infty B^0_{\infty,1}}\|\theta\|^2_{L_t^\infty B^1_{\infty,1}}. \end{aligned} \tag{4.14}$$

We then estimate $B_{n,1,II}$. According to (4.11) and (4.12), then we have

$$B_{n,1,II} = \int_{t_n}^{t_{n+1}} \Delta_j e^{-\nu(t_{n+1}-s)\Lambda^\gamma}\left(e^{-\nu(s-t_n)\Lambda^\gamma}\nabla^\perp\Lambda^{-1}\theta(t_n)\cdot\nabla V(s)\right)\ \mathrm{ds}\,.$$

By similar arguments we arrive at

$$\sum_j \|B_{n,1,II}\|_{L^\infty} \lesssim \tau\|\theta\|_{L_t^\infty B^0_{\infty,1}}\|V\|_{L_t^\infty B^1_{\infty,1}}. \tag{4.15}$$

Similar to (4.13) we can bound $\|V\|_{L_t^\infty B^1_{\infty,1}}$ by applying Lemma 2.4 and the product rule:

$$\|V(s)\|_{B^1_{\infty,1}} \lesssim \tau\left(\|\theta\|^2_{L_t^\infty B^1_{\infty,1}} + \|\theta\|_{L_t^\infty B^0_{\infty,1}}\|\theta\|_{L_t^\infty B^2_{\infty,1}}\right). \tag{4.16}$$

Combining (4.14), (4.15) and (4.16) we get

$$\sum_j \|B_{n,1}\|_{L^\infty} \lesssim \tau^2 \left(\|\theta\|_{L_t^\infty B^0_{\infty,1}} \|\theta\|^2_{L_t^\infty B^1_{\infty,1}} + \|\theta\|^2_{L_t^\infty B^0_{\infty,1}} \|\theta\|_{L_t^\infty B^2_{\infty,1}}\right). \tag{4.17}$$

We proceed to estimate the term $B_{n,2}$. Recall that

$$B_{n,2} = \int_{t_n}^{t_{n+1}} h(s) - h(t_{n+1})\, \mathrm{ds},$$

where $h(s) = \Delta_j e^{-\nu(t_{n+1}-s)\Lambda^\gamma}(\nabla^\perp \Lambda^{-1} v(s) \cdot \nabla v(s))$, with $v(s) = e^{-\nu(s-t_n)\Lambda^\gamma}\theta(t_n)$. Note that we can approximate $B_{n,2}$ by $\partial_s h$ and therefore we derive that

$$\begin{aligned}\partial_s h(s) =& \nu e^{-\nu(t_{n+1}-s)\Lambda^\gamma} \Delta_j \Lambda^\gamma (\nabla^\perp \Lambda^{-1} v \cdot \nabla v)\\ &- \nu e^{-\nu(t_{n+1}-s)\Lambda^\gamma} \Delta_j (\Lambda^\gamma \nabla^\perp \Lambda^{-1} v \cdot \nabla v) - \nu e^{-\nu(t_{n+1}-s)\Lambda^\gamma} \Delta_j (\nabla^\perp \Lambda^{-1} v \cdot \nabla \Lambda^\gamma v)\\ =& \nu e^{-\nu(t_{n+1}-s)\Lambda^\gamma} [\Delta_j \Lambda^\gamma, \nabla^\perp \Lambda^{-1} v \cdot \nabla] v - \nu e^{-\nu(t_{n+1}-s)\Lambda^\gamma} \Delta_j (\Lambda^\gamma \nabla^\perp \Lambda^{-1} v \cdot \nabla v)\\ &- \nu e^{-\nu(t_{n+1}-s)\Lambda^\gamma} [\Delta_j, \nabla^\perp \Lambda^{-1} v \cdot \nabla] \Lambda^\gamma v.\end{aligned} \tag{4.18}$$

By the Besov commutator Lemma 2.3 we can conclude

$$\begin{aligned}\sum_j \|[\Delta_j \Lambda^\gamma, \nabla^\perp \Lambda^{-1} v \cdot \nabla] v\|_{L^\infty} &\lesssim \|v\|_{B^1_{\infty,1}} \|v\|_{B^\gamma_{\infty,1}},\\ \sum_j \|[\Delta_j, \nabla^\perp \Lambda^{-1} v \cdot \nabla] \Lambda^\gamma v\|_{L^\infty} &\lesssim \|v\|_{B^1_{\infty,1}} \|v\|_{B^\gamma_{\infty,1}}.\end{aligned} \tag{4.19}$$

For the remaining term we apply the Lemma 2.4 that

$$\sum_j \|\Delta_j (\Lambda^\gamma \nabla^\perp \Lambda^{-1} v \cdot \nabla v)\|_{L^\infty} \lesssim \|v\|_{B^\gamma_{\infty,1}} \|v\|_{B^1_{\infty,1}}. \tag{4.20}$$

Combining the estimates (4.18), (4.19) and (4.20) we can conclude that

$$\sum_j \|B_{n,2}\|_{L^\infty} \lesssim \tau^2 \nu \|v\|_{B^\gamma_{\infty,1}} \|v\|_{B^1_{\infty,1}} \lesssim \tau^2 \nu \|\theta\|_{L_t^\infty B^\gamma_{\infty,1}} \|\theta\|_{L_t^\infty B^1_{\infty,1}}. \tag{4.21}$$

Note that $\gamma \in (0, 2]$ by assumption, therefore (4.21) can be reduced to

$$\sum_j \|B_{n,2}\|_{L^\infty} \lesssim \tau^2 \nu \|\theta\|_{L_t^\infty B^2_{\infty,1}} \|\theta\|_{L_t^\infty B^1_{\infty,1}}. \tag{4.22}$$

Lastly, to estimate $B_{n,3}$ we recall that (4.10)

$$B_{n,3} = \tau \Delta_j \left(\nabla^\perp \Lambda^{-1} e^{-\nu\tau\Lambda^\gamma} \theta(t_n) \cdot \nabla V(t_{n+1})\right).$$

Then by Lemma 2.4 and noting that $\operatorname{div} \nabla^\perp \Lambda^{-1} e^{-\nu\tau\Lambda^\gamma}\theta = 0$, we have

$$\begin{aligned}\sum_j \|B_{n,3}\|_{L^\infty} \lesssim& \tau \|\nabla^\perp \Lambda^{-1} \theta\|_{L_t^\infty B^0_{\infty,1}} \|V(t_{n+1})\|_{B^1_{\infty,1}}\\ \lesssim& \tau^2 \left(\|\theta\|^2_{L_t^\infty B^0_{\infty,1}} \|\theta\|_{L_t^\infty B^2_{\infty,1}} + \|\theta\|_{L_t^\infty B^0_{\infty,1}} \|\theta\|^2_{L_t^\infty B^1_{\infty,1}}\right).\end{aligned} \tag{4.23}$$

Taking $\operatorname{sgn}(\Delta_j \mathcal{E}^{n+1})|\Delta_j \mathcal{E}^{n+1}|^{p-1}$ as a test function of (4.9), we can then obtain the following energy estimate:

$$\begin{aligned}\|\Delta_j \mathcal{E}^{n+1}\|_{L^p} \le& \|\Delta_j \mathcal{E}^n\|_{L^p} + \tau \|\Delta_j \left(e^{-\nu\tau\Lambda^\gamma} \nabla^\perp \Lambda^{-1} \mathcal{E}^n \cdot \nabla \theta(t_{n+1})\right)\|_{L^p}\\ &+ \tau \left\| \left[e^{-\nu\tau\Lambda^\gamma} \nabla^\perp \Lambda^{-1} \theta^n \cdot \nabla, \Delta_j\right] \mathcal{E}^{n+1} \right\|_{L^p} + \|B_{n,1}\|_{L^p} + \|B_{n,2}\|_{L^p} + \|B_{n,3}\|_{L^p}.\end{aligned}$$

Letting $p \to \infty$ and summing in j we have

$$\|\mathcal{E}^{n+1}\|_{B^0_{\infty,1}} \leq \|\mathcal{E}^n\|_{B^0_{\infty,1}} + C\tau(\|\mathcal{E}^n\|_{B^0_{\infty,1}}\|\theta\|_{L^\infty_t B^1_{\infty,1}} + \|\theta^n\|_{B^1_{\infty,1}}\|\mathcal{E}^{n+1}\|_{B^0_{\infty,1}}) + \sum_{i=1}^{3}\sum_{j}\|B_{n,i}\|_{L^\infty}$$

by applying Lemma 2.3, Lemma 2.4 and Lemma 2.5. Note that by Theorem 1.4, $\|\theta^n\|_{B^1_{\infty,1}} \lesssim 1$ and recall (4.17), (4.22) and (4.23) we thus obtain that

$$\|\mathcal{E}^{n+1}\|_{B^0_{\infty,1}} \leq \frac{1+C^*\tau}{1-C^*\tau}\|\mathcal{E}^n\|_{B^0_{\infty,1}} + \frac{C^*(1+\nu)\tau^2}{1-C^*\tau},$$

where C^* depends on the displayed exact-solution norms; the factor $1+\nu$ is uniformly bounded for $0 \leq \nu \leq \nu_{\max}$. By the discrete Grönwall's inequality (cf. Cheng et al., 2024a) we arrive at

$$\sup_n \|\mathcal{E}^n\|_{B^0_{\infty,1}} \lesssim \tau,$$

where we only need the endpoint requirement that

$$\theta \in C([0,T]; L^2(\mathbb{T}^2)) \cap L^\infty(0,T; B^2_{\infty,1}(\mathbb{T}^2)).$$

This ends the proof of Theorem 1.5.

5. Full Discretization by the Fourier Spectral Method

In order to solve the (SQG) equations while handling the challenging non-local operators $\nabla^\perp\Lambda^{-1}$ and Λ^γ, we implement the LRI with the following fully discrete Fourier spectral method:

$$\begin{cases} \theta^{n+1} = e^{-\nu\tau\Lambda^\gamma}\theta^n - \tau\Pi_N(e^{-\nu\tau\Lambda^\gamma}u^n\cdot\nabla\theta^{n+1}), \\ u^n = \nabla^\perp\Lambda^{-1}\theta^n, \\ \theta^0 = \Pi_N\theta_0, \end{cases} \tag{5.1}$$

where τ is the time step. For $N \geq 2$, we introduce the space

$$X_N = \operatorname{span}\left\{\cos(k\cdot x)\ ,\ \sin(k\cdot x):\quad k=(k_1,k_2)\in\mathbb{Z}^2\ ,\ |k|_\infty = \max\{|k_1|,|k_2|\}\in[1,N]\right\}.$$

We thus define Π_N to be the truncation operator of Fourier modes $1 \leq |k|_\infty \leq N$, namely the Fourier modes are no larger than N and the zero-th mode is projected off. Note that $\Pi_N\theta_0 \in X_N$ and therefore by induction we have $\theta^n \in X_N$,$\forall n \geq 0$. In addition we can further derive that $\operatorname{div} u^n = 0$ for all n by the definition of u^n. Recall that the frequency cut-off operator S_j defined in (2.1), essentially $S_j = \Pi_{2^{j+1}}$ in our setting. Then we have the following error estimates for the Fourier spectral method.

Theorem 5.1 (Fully discretized error estimates)**.** Assume that $\theta(t,x)$ is the exact solution to (SQG).

(i) **L^2-error:** Assume $\theta(t) \in H^{2+\epsilon}(\mathbb{T}^2)$ for any sufficiently small $\epsilon > 0$. Then the following L^2-error estimate holds.

$$\sup_n \|\theta^{n+1} - \theta(t_{n+1})\|_{L^2} \leq C_1(\tau + N^{-1-\epsilon}). \tag{5.2}$$

(ii) **$B^0_{\infty,1}$-error:** Assume $\theta(t) \in B^2_{\infty,1}(\mathbb{T}^2)$. Then the following $B^0_{\infty,1}$-error estimate holds.

$$\sup_n \|\theta^{n+1} - \theta(t_{n+1})\|_{B^0_{\infty,1}} \leq C_2(\tau + N^{-1}). \tag{5.3}$$

For every fixed $\nu_{\max} > 0$, the constants $C_1, C_2 > 0$ depend on T, $\nu_{\max}$, and the indicated exact-solution norms, but are independent of $\nu \in [0,\nu_{\max}]$ and $\gamma \in (0,2]$.

Remark 5.2. Theorem 5.1 displays the same endpoint distinction as the time-discrete analysis: the Sobolev estimate uses an additional ϵ derivative, while the Besov estimate is formulated at derivative index two. This is an endpoint comparison, not a claim that $B^2_{\infty,1}$ is a larger space than $H^{2+\epsilon}$ or $W^{2,2+\epsilon}$; see also (Li et al., 2022).

6. Numerical Experiments

In this section, we present numerical evidence including the dynamics, the rate of vanishing viscosity and the order of error. In this section we fix $\gamma = 2, N_x = N_y = 128$ to be the hyperparameter. Note that even though $\Lambda^2 = -\Delta$ seems to be a local differential operator, the equation $u = \nabla^\perp\Lambda^{-1}\theta$ guarantees the non-local behavior of the SQG system.

6.1. Convergence test: $L^2, L^\infty, B^0_{\infty,1}-$errors with fixed ν.

In this subsection we present the error of the LRI (1.1). Throughout this subsection we choose the following initial data suggested by (Cheng et al., 2024a,b) and (Li et al., 2022):

$$\theta_0 = -\frac{m}{2}(\cos(\frac{x}{2}))^m(\cos(\frac{y}{2}))^{m-1}\sin(\frac{y}{2}),$$

For this family of initial data, the dominant singularity occurs at $y = \pm\pi$, where $|\theta_0|$ is proportional to d_y^{m-1}, with d_y denoting the distance to the periodic seam. Consequently, up to but not including the endpoints, $\theta_0 \in H^s$ for every $s < m - \frac{1}{2}$, whereas $\theta_0 \in B^s_{\infty,1}$ for every $s < m - 1$. Thus $m = 1.8$ and $m = 2.8$ correspond to Sobolev regularities $H^{1.3-}$ and $H^{2.3-}$, respectively, but they should not be identified with $B^{1+}_{\infty,1}$ and $B^{2+}_{\infty,1}$. We use these values as representative finite-regularity profiles with a 0.3-derivative margin above Sobolev orders one and two. This margin keeps the nonsmooth profiles adequately resolved at the fixed Fourier resolution $N = 128$ and permits a clean comparison of the temporal convergence and stability of the three methods. The experiments are not intended to realize the exact function-space endpoints or to numerically establish the sharpness of the endpoint Besov theorem.

We shall generate the "accurate" reference solution θ_R by computing using the same schemes but with $\tau = 10^{-6}$. We then compare the numerical solutions of our LRI (1.1) to the reference solution θ_R under different choices of τ-values. Similar comparison will be done for 1st order IMEX method (Cheng, 2026; Cheng et al., 2024a) and the usual exponential integrator (EI) method (Cheng et al., 2026a). More specifically speaking, the schemes are given below:

$$\begin{cases} \frac{\theta^{n+1}-\theta^n}{\tau} + u^n \cdot \nabla\theta^{n+1} = -\nu\Lambda^\gamma\theta^{n+1}, \\ u^n = \nabla^\perp\Lambda^{-1}\theta^n, \end{cases} \tag{IMEX}$$

and

$$\begin{cases} \theta^{n+1} = e^{-\nu\tau\Lambda^\gamma}\theta^n - \frac{1-e^{-\tau\nu\Lambda^\gamma}}{\nu\Lambda^\gamma}(u^n \cdot \nabla\theta^n), \\ u^n = \nabla^\perp\Lambda^{-1}\theta^n. \end{cases} \tag{EI}$$

In this first numerical experiment we compute the SQG model (SQG) using the LRI (1.1), IMEX (IMEX) and exponential integrator method (EI). We fix $\gamma = 2, N_x = N_y = 128$ and vary the time step $\tau = \frac{0.01}{2^k}$ for $k = 0, 1, \cdots, 7$. The local residual is fixed to be 1e-13 in the iteration scheme (A.5). The $L^2, L^\infty, B^0_{\infty,1}$ differences at $T = 0.1$ with $\nu = 0.1$ and $m = 1.8$ are presented in Table 1. It is clear that their differences are of order $O(\tau)$ as $\tau \to 0$. The observed errors in all three lower-regularity norms exhibit first-order behavior in τ, consistently with the convergence analysis. In view of the regularity characterization above, however, this finite-resolution experiment is not presented as a direct numerical verification of the endpoint assumptions in Proposition 1.2 or Theorem 1.5.

Table 1. Errors for fixed $\nu = 0.1$ and varying τ.

$\tau = 0.01$	L^2-error	L^∞-error	$B^0_{\infty,1}$-error
τ	9.589e-06	7.324e-06	2.124e-05
$\tau/2$	4.796e-06	3.664e-06	1.062e-05
$\tau/4$	2.399e-06	1.833e-06	5.313e-06
$\tau/8$	1.200e-06	9.169e-07	2.658e-06
$\tau/16$	6.002e-07	4.590e-07	1.330e-06
$\tau/32$	3.005e-07	2.300e-07	6.665e-07
$\tau/64$	1.506e-07	1.156e-07	3.346e-07
$\tau/128$	7.569e-08	5.845e-08	1.687e-07

We present the L^∞-errors of the LRI, IMEX, and EI methods with $m = 1.8, 2.8$ and $\nu = 0.1, 0.01, 0.0001$ in Figure 1. It is clear that the usual EI method is not as stable as the other two methods with larger time step when the viscosity ν is small.

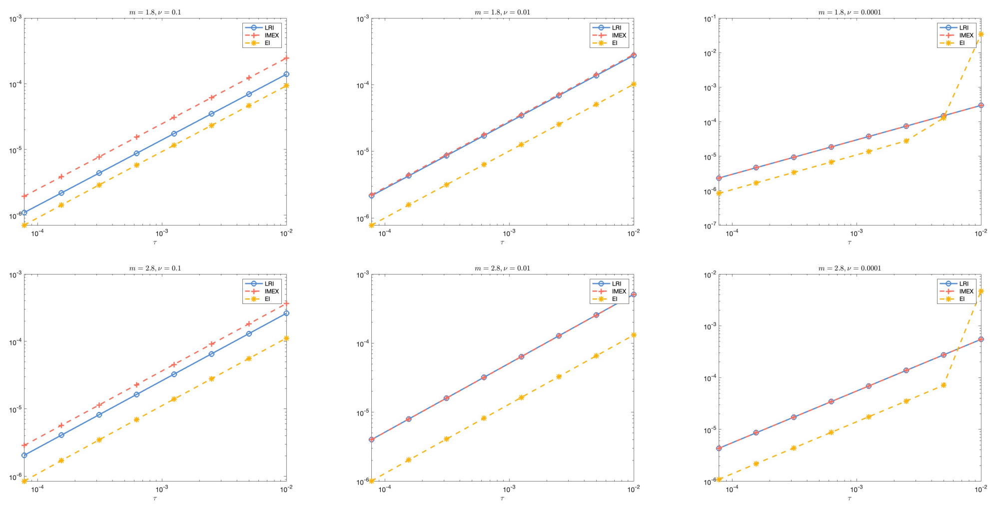

Figure 1. Convergence test for the LRI (1.1). We choose $\nu = 0.1, 0.01, 0.0001$ and vary the time step τ. The first row uses $m = 1.8$ in the initial data, and the second row uses $m = 2.8$.

Remark 6.1. It is worth introducing the discrete version of Besov norm $B^0_{\infty,1}$ here (defined in (2.2) from Section 2). In order to compute $\|f\|_{B^0_{\infty,1}}$ numerically for any function f, it is essential to compute $\|\Delta_j f\|_{L^\infty}$ for $j = 0, 1, \cdots, K$, where $2^K = N$ from the Fourier side. Then we sum in j to get the desired norm.

6.2. **Rate of vanishing viscosity.** In this subsection we present the rate of vanishing viscosity of the LRI (1.1). Throughout this subsection we choose the following initial data suggested by (Cheng et al., 2024a,b) and (Li et al., 2022):

$$\theta_0 = -\frac{m}{2}(\cos(\frac{x}{2}))^m(\cos(\frac{y}{2}))^{m-1}\sin(\frac{y}{2}),$$

As characterized in the preceding subsection, $m = 1.8$ yields $H^{1.3-}$ Sobolev regularity (and $B^{0.8-}_{\infty,1}$ Besov regularity), while $m = 2.8$ yields $H^{2.3-}$ (and $B^{1.8-}_{\infty,1}$). These values are finite-regularity representatives rather than exact borderline parameters. We shall first generate the "accurate" reference solution θ_R by computing using the same schemes but with $\tau = 10^{-6}$ and fixing $\nu = 0, \gamma = 2$. We then compare the numerical solutions of our LRI (1.1) to the reference solution θ_R under different choices of ν-values.

In this second numerical experiment we compute the SQG model (SQG) using (1.1). We fix $\tau = 10^{-5}, N_x = N_y = 128$ and we vary the viscosity $\nu = \frac{0.001}{2^k}$ for $k = 0, 1, \cdots, 7$. The local residual is fixed to be 1e-13 in the iteration scheme (A.5). The $L^2, L^\infty, B^0_{\infty,1}$ differences at $T = 0.1$ are presented in Table 2. It is clear that these differences are linear in ν as $\nu \to 0$. We see that all the errors in the lower-regularity norms behave as $O(\nu)$, as predicted by Theorem 1.1 of Cheng et al. (2026b). However, in practice it is not easy to capture the exact rate $\nu^{\min\{1,\frac{1}{\gamma}\}}$. The main reason is due to the difficulty to construct solutions of the exact regularity. Another challenge is that spatial or frequency discretization requires higher regularity for the convergence of the numerical scheme. See also Figure 2.

$\nu = 0.001$	L^2-error	L^∞-error	$B^0_{\infty,1}$-error
ν	3.576e-04	5.909e-04	1.426e-03
$\nu/2$	1.817e-04	3.032e-04	7.291e-04
$\nu/4$	9.162e-05	1.537e-04	3.687e-04
$\nu/8$	4.601e-05	7.734e-05	1.854e-04
$\nu/16$	2.306e-05	3.880e-05	9.298e-05
$\nu/32$	1.154e-05	1.943e-05	4.656e-05
$\nu/64$	5.775e-06	9.726e-06	2.330e-05
$\nu/128$	2.889e-06	4.866e-06	1.166e-05

Table 2. Errors for fixed $\tau = 10^{-5}$ and varying ν.

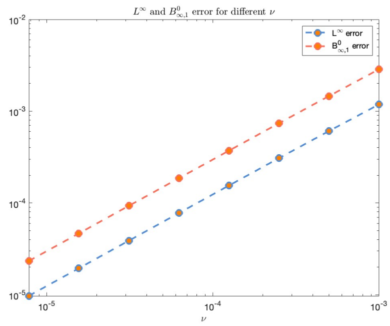

Figure 2. Rate of the vanishing viscosity for the LRI (1.1) with $\tau = 10^{-5}$ fixed and ν varying.

6.3. **Dynamics.** In this subsection we present dynamics of the SQG equations on two benchmark examples.

6.3.1. *Vortex Waltz.* In this example we consider the following initial data of two Gaussian vortices. The initial data is given as

$$\theta_0 = \nabla^\perp \cdot \vec{u_0} = \exp(-5((x + \frac{\pi}{4})^2 + y^2)) + \exp(-5((x - \frac{\pi}{4})^2 + y^2)). \tag{6.1}$$

We present the dynamics of θ with the initial data given in (6.1) after zero-mean projection. We present the θ with fixed $\nu = 0.0001$ in Figure 3 and 4. This benchmark example is motivated by (Cheng et al., 2024a,b). To be more specific in (Cheng et al., 2024a), dynamics of 2D incompressible Navier-Stokes (NS) are studied; indeed there are some similarities between the SQG equations and the vorticity equation of the NS system as can be shown in the dynamics. From the dynamics we can observe that when the viscosity ν is small the dynamics of the two Gaussian vortices tend to merge as they orbit around each other. Indeed on the contrary, while the viscosity ν is larger the dynamics tend to be more stable. We see that the frequency resolution does not contribute to a major difference in the dynamics of the vortex Waltz.

6.3.2. *Dynamics of blow-up initial data.* In this example we consider the following initial data:

$$\theta_0 = -\frac{m}{2}(\cos(\frac{x}{2}))^m(\cos(\frac{y}{2}))^{m-1}\sin(\frac{y}{2}), \tag{6.2}$$

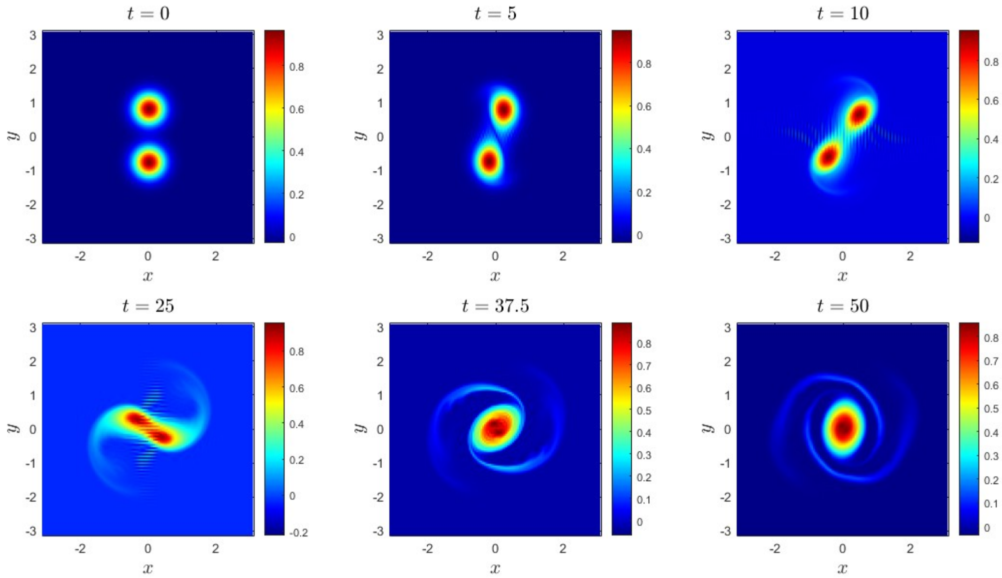

Figure 3. Dynamics of vortex Waltz with $N = 128$.

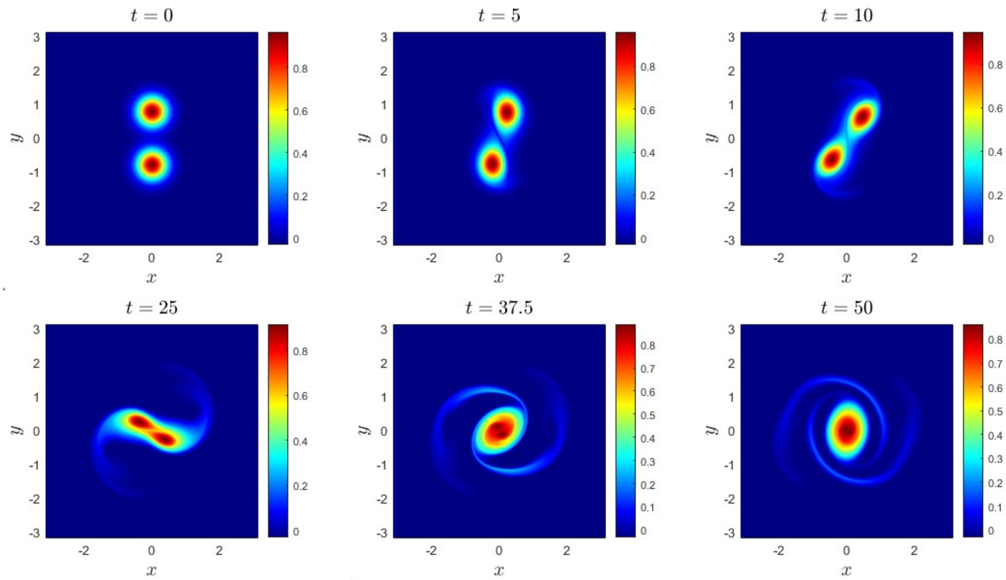

Figure 4. Dynamics of vortex Waltz with $N = 1024$.

where $m = 0.8$ and we choose viscosity $\nu = 0.1$. It is clear that the data θ_0 from (6.2) is in H^s for $s < 0.3$. Moreover $\theta \notin L^\infty$; we can observe that singularities are located at $y = \pm\pi$. Therefore one may treat it as a special blow-up initial data. The Figures 5 and 6 present the dynamics of SQG equations after certain types of L^∞ blow-up. The viscosity makes the system more stable and smoother even for this blow-up-type initial data. We also emphasize here that the initial data is of mean zero, even in x and odd in y. From the Figures 5 and 6 we clearly see the differences in the dynamics between $N = 128$ and $N = 1024$ cases. Moreover according to the error estimate, the frequency truncation error is $O(N^{-s})$. The values $128^{-0.3} \approx 0.233$ and $1024^{-0.3} \approx 0.125$ do not differ by an order of magnitude. Indeed this difference suggests energy cascade: energy transfer from low frequency (large scale) to high frequency (small scale). As one can tell in the $N = 128$ (low frequency) case, the convection dominates the dynamics and therefore turbulence tends to occur in short time; smoothing effect by the viscosity then stabilizes the system.

As for the $N = 1024$ (high frequency) case, the viscosity dominates the dynamics and therefore the system remains stable for all times.

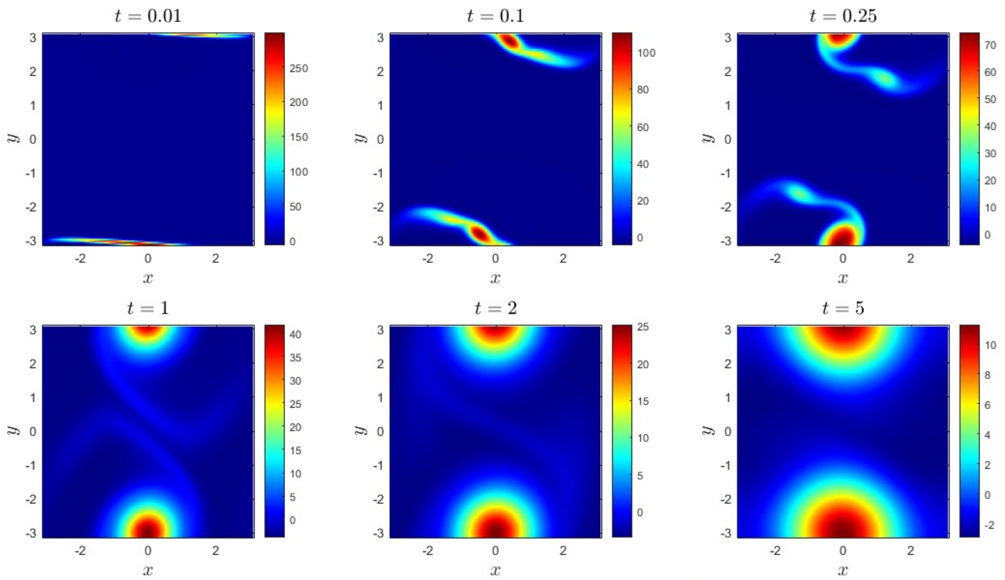

Figure 5. Dynamics of blow-up initial data with $N = 128$.

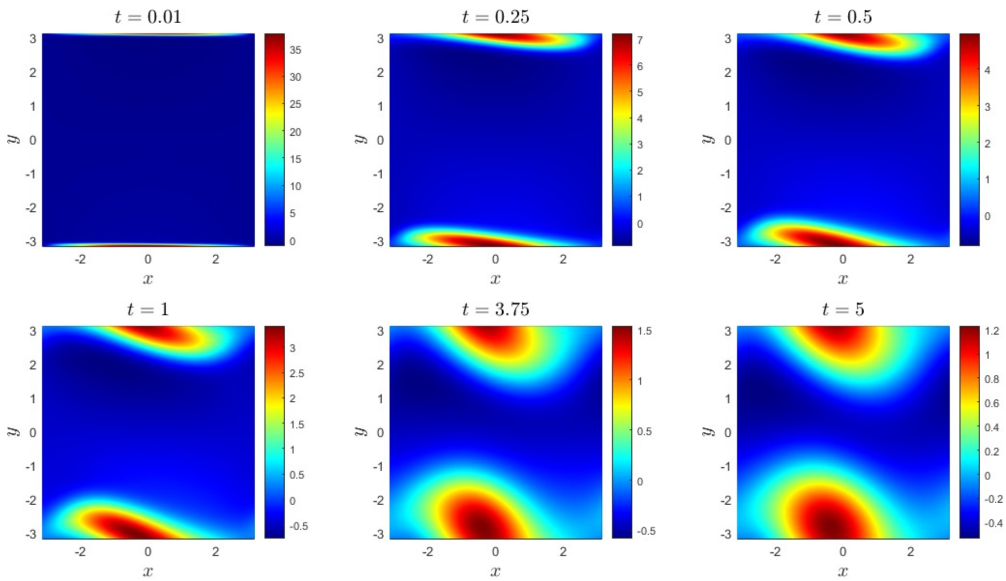

Figure 6. Dynamics of blow-up initial data with $N = 1024$.

7. Concluding Remarks

In this paper, we have proposed and rigorously analyzed a novel semi-implicit low-regularity integrator (LRI) for the (dissipative) surface quasi-geostrophic (SQG) equations. A central mathematical challenge in the numerical analysis of active scalars is the severe derivative loss induced by the highly singular non-local convection term, which traditionally forces sub-optimal, artificially high regularity assumptions in classical Sobolev-based error estimates.

To fundamentally bypass this structural barrier, we introduced a tailored numerical Besov space framework. By exploiting the special quasi-algebraic div-curl structures and refined commutator estimates within the critically embedded space $B^0_{\infty,1}$, we successfully established unconditional energy stability and sharp, first-order temporal error estimates. Our analysis reaches the endpoint derivative index $\theta \in L^\infty(0,T;B^2_{\infty,1})$ and eliminates the fractional derivative surplus in the Sobolev calculation. As emphasized in Remark 1.6, this is an endpoint, derivative-loss improvement rather than an inclusion-wise weakening of the Sobolev hypothesis. These theoretical findings were strongly corroborated by extensive numerical experiments, including rigorous convergence tests and the robust simulation of singular vortex patch dynamics.

The mathematical framework developed herein extends significantly beyond the 2D SQG model. The transition from classical Sobolev energy methods to Besov calculus provides a robust and universal paradigm for the sharp numerical analysis of general incompressible fluids. Future research directions include extending this numerical Besov framework to higher-order low-regularity integrators and applying it to the 3D Navier–Stokes and Euler equations.

Acknowledgement

X. Cheng is partially supported by NSFC (Grants No. 12401270 and No. 42450192), Natural Science Foundation of Shanghai (Grant No. 24ZR1404200) and Shanghai Magnolia Talent Plan Pujiang Project (Grant No. 24PJA007). S. Wang is partially supported by the China National Postdoctoral Program for Innovative Talents (Grant No. 20250061) and China Postdoctoral Science Foundation (Grant No. 2024M760058).

Appendix A. Proof of Theorem 5.1

Proof of Theorem 5.1. We first show (5.2). In particular, we have

$$\begin{aligned}\theta(t_{n+1}) =& e^{-\nu\tau\Lambda^\gamma}\theta(t_n) - \int_{t_n}^{t_{n+1}} e^{-\nu(t_{n+1}-s)\Lambda^\gamma}\Pi_N\left(\nabla^\perp\Lambda^{-1}\theta\cdot\nabla\theta\right)(s)\,\mathrm{ds}\\ &- \int_{t_n}^{t_{n+1}} e^{-\nu(t_{n+1}-s)\Lambda^\gamma}(I-\Pi_N)\left(\nabla^\perp\Lambda^{-1}\theta\cdot\nabla\theta\right)(s)\,\mathrm{ds}\,.\end{aligned}$$

We then denote $\mathcal{E}^{n+1} = \theta^{n+1} - \theta(t_{n+1})$ to be the error. Similar to the arguments in previous sections, we infer from (5.1) that

$$\begin{aligned}\mathcal{E}^{n+1} + \tau\Pi_N\left(e^{-\nu\tau\Lambda^\gamma}\nabla^\perp\Lambda^{-1}\theta^n\cdot\nabla\mathcal{E}^{n+1}\right) =& e^{-\nu\tau\Lambda^\gamma}\mathcal{E}^n - \tau\Pi_N\left(e^{-\nu\tau\Lambda^\gamma}\nabla^\perp\Lambda^{-1}\mathcal{E}^n\cdot\nabla\theta(t_{n+1})\right)\\ &+ \widetilde{R}_{n,1} + \widetilde{R}_{n,2} + \widetilde{R}_{n,3} + \widetilde{R}_{n,4},\end{aligned}\tag{A.1}$$

where the remaining terms $\widetilde{R}_{n,j}, j = 1,2,3,4$ are defined as follows:

$$\begin{aligned}\widetilde{R}_{n,1} =& \int_{t_n}^{t_{n+1}} e^{-\nu(t_{n+1}-s)\Lambda^\gamma}\Pi_N\left(\nabla^\perp\Lambda^{-1}(\theta(s) - e^{-\nu(s-t_n)\Lambda^\gamma}\theta(t_n))\cdot\nabla\theta(s)\right)\mathrm{ds}\\ &+ \int_{t_n}^{t_{n+1}} e^{-\nu(t_{n+1}-s)\Lambda^\gamma}\Pi_N\left(\nabla^\perp\Lambda^{-1}e^{-\nu(s-t_n)\Lambda^\gamma}\theta(t_n)\cdot\nabla(\theta(s) - e^{-\nu(s-t_n)\Lambda^\gamma}\theta(t_n))\right)\mathrm{ds},\end{aligned}$$

and

$$\widetilde{R}_{n,2} = \int_{t_n}^{t_{n+1}} \widetilde{g}(s) - \widetilde{g}(t_{n+1})\,\mathrm{ds},$$

where $\widetilde{g}(s) = e^{-\nu(t_{n+1}-s)\Lambda^\gamma}\Pi_N(\nabla^\perp\Lambda^{-1}v(s)\cdot\nabla v(s))$, with $v(s) = e^{-\nu(s-t_n)\Lambda^\gamma}\theta(t_n)$. Moreover, we denote

$$\begin{aligned}\widetilde{R}_{n,3} &= \tau\Pi_N\left(\nabla^\perp\Lambda^{-1}e^{-\nu\tau\Lambda^\gamma}\theta(t_n)\cdot\nabla(e^{-\nu\tau\Lambda^\gamma}\theta(t_n)-\theta(t_{n+1}))\right)\\ &= \tau\Pi_N\left(\nabla^\perp\Lambda^{-1}e^{-\nu\tau\Lambda^\gamma}\theta(t_n)\cdot\nabla\int_{t_n}^{t_{n+1}}e^{-\nu(t_{n+1}-s)\Lambda^\gamma}(\nabla^\perp\Lambda^{-1}\theta(s)\cdot\nabla\theta(s))\,\mathrm{ds}\right).\end{aligned}$$

and

$$\widetilde{R}_{n,4} = \int_{t_n}^{t_{n+1}} e^{-\nu(t_{n+1}-s)\Lambda^\gamma}(I-\Pi_N)\left(\nabla^\perp\Lambda^{-1}\theta\cdot\nabla\theta\right)(s)\,\mathrm{ds}\,. \tag{A.2}$$

In fact, the estimates of $\widetilde{R}_{n,j}, j = 1,2,3$ are completely parallel to $R_{n,j}, j = 1,2,3$. Similarly, we can estimate $\widetilde{R}_{n,4}$ from (A.2) as below:

$$\begin{aligned}\|\widetilde{R}_{n,4}\|_{L^2} &\lesssim \tau\sum_{2^j\geq N}\|\Delta_j(\nabla^\perp\Lambda^{-1}\theta\cdot\nabla\theta)\|_{L^\infty_t L^2}\\ &\lesssim \tau N^{-1-\epsilon}\sum_{2^j\geq N}\|\Delta_j\Lambda^{1+\epsilon}(\nabla^\perp\Lambda^{-1}\theta\cdot\nabla\theta)\|_{L^\infty_t L^2}\\ &\lesssim \tau N^{-1-\epsilon}\|\theta\|^2_{L^\infty_t H^{2+\epsilon}}.\end{aligned} \tag{A.3}$$

We also take the L^2-inner product between (A.1) and $\mathcal{E}^{n+1}$. Note that $\operatorname{div}\nabla^\perp\Lambda^{-1}\theta^n = 0$, we therefore obtain that

$$\begin{aligned}\|\mathcal{E}^{n+1}\|^2_{L^2} &= \left(e^{-\nu\tau\Lambda^\gamma}\mathcal{E}^n,\mathcal{E}^{n+1}\right) - \tau\left(e^{-\nu\tau\Lambda^\gamma}\nabla^\perp\Lambda^{-1}\mathcal{E}^n\cdot\nabla\theta(t_{n+1}),\mathcal{E}^{n+1}\right)\\ &\quad+\left(\widetilde{R}_{n,1}+\widetilde{R}_{n,2}+\widetilde{R}_{n,3}+\widetilde{R}_{n,4},\mathcal{E}^{n+1}\right)\\ &\leq\frac{1}{2}\|\mathcal{E}^n\|^2_{L^2}+\frac{1}{2}\|\mathcal{E}^{n+1}\|^2_{L^2}+C\tau\|\nabla\theta(t_{n+1})\|_{L^\infty}\|\mathcal{E}^n\|_{L^2}\|\mathcal{E}^{n+1}\|_{L^2}+C\tau^2\|\mathcal{E}^{n+1}\|_{L^2}\\ &\quad+C\nu\tau^2\|\mathcal{E}^{n+1}\|_{L^2}+C\tau N^{-1}\|\mathcal{E}^{n+1}\|_{L^2}\\ &\leq\frac{1}{2}\|\mathcal{E}^n\|^2_{L^2}+\frac{1}{2}\|\mathcal{E}^{n+1}\|^2_{L^2}+C\tau\|\mathcal{E}^n\|^2_{L^2}+C\tau\|\mathcal{E}^{n+1}\|^2_{L^2}+C\tau^3+C\nu^2\tau^3+C\tau N^{-2-2\epsilon}.\end{aligned} \tag{A.4}$$

So we can derive from (A.4) and (A.3) that

$$\|\mathcal{E}^{n+1}\|^2_{L^2}\leq\frac{1+C^*\tau}{1-C^*\tau}\|\mathcal{E}^n\|^2_{L^2}+\frac{C^*(1+\nu^2)\tau^3}{1-C^*\tau}+\frac{C^*\tau N^{-2-2\epsilon}}{1-C^*\tau}.$$

Then by the discrete Grönwall's inequality we can conclude (5.2). The proof of (5.3) is very similar. The main difference is to control $\sum_j\|\widetilde{B}_{n,4}\|_{L^\infty}$, where

$$\widetilde{B}_{n,4} = \int_{t_n}^{t_{n+1}} e^{-\nu(t_{n+1}-s)\Lambda^\gamma}\Delta_j(I-\Pi_N)\left(\nabla^\perp\Lambda^{-1}\theta\cdot\nabla\theta\right)(s)\,\mathrm{ds}\,.$$

Indeed we have

$$\sum_j\|\widetilde{B}_{n,4}\|_{L^\infty}\lesssim\tau N^{-1}\left(\|\theta\|_{L^\infty_t B^0_{\infty,1}}\|\theta\|_{L^\infty_t B^2_{\infty,1}}+\|\theta\|_{L^\infty_t B^0_{\infty,1}}\|\theta\|_{L^\infty_t B^1_{\infty,1}}\right).$$

Therefore, we can derive the following error estimate:

$$\|\mathcal{E}^{n+1}\|_{B^0_{\infty,1}}\leq\frac{1+C^*\tau}{1-C^*\tau}\|\mathcal{E}^n\|_{B^0_{\infty,1}}+\frac{C^*(1+\nu)\tau^2}{1-C^*\tau}+\frac{C^*\tau N^{-1}}{1-C^*\tau},$$

which proves (5.3).

□

In practice our LRI is implemented via the following iteration:

$$\begin{cases} \theta^{(m+1)} = e^{-\nu\tau\Lambda^\gamma}\theta^n - \tau\Pi_N(e^{-\nu\tau\Lambda^\gamma}u^n \cdot \nabla\theta^{(m)}), \\ u^n = \nabla^\perp\Lambda^{-1}\theta^n, \\ \theta^0 = \Pi_N\theta_0, \end{cases} \tag{A.5}$$

Here at each time step n we implement an iteration of $\theta^{(m)}$ with $\theta^{(0)} = \theta^n$ and eventually $\theta^{(m)}$ converges. We therefore define $\lim_m \theta^{(m)} = \theta^{n+1}$ up to a local tolerance and therefore the iteration is finite. Such iteration (A.5) converges; we refer the readers to Cheng et al. (2024a) for the details in the Navier-Stokes case and we omit the proof here.

References

Abdo, E., Hu, R. and Lin, Q. Neural network solutions to the critical SQG equations via approximating nonlocal periodic operators. *Physica D: Nonlinear Phenomena*, 476: 134652, 2025.

Bae, H. and Granero-Belinchón, R. Global existence for some transport equations with nonlocal velocity. *Adv. Math.*, 269: 197–219, 2015.

Bahouri, H., Chemin, J. Y. and Danchin, R. Fourier analysis and nonlinear partial differential equations, *Springer, Heidelberg*, 2011.

Bai, G., Li, B. and Wu, Y. A constructive low-regularity integrator for the 1d cubic nonlinear Schrödinger equation under the Neumann boundary condition. *IMA J. Numer. Anal.*, 43(6): 3243–3281, 2023.

Bonito, A. and Nazarov, M. Numerical simulations of surface quasi-geostrophic flows on periodic domains. *SIAM Journal on Scientific Computing*, 43(2): B405-B430, 2021.

Buckmaster, T., Shkoller, S. and Vicol, V. Nonuniqueness of weak solutions to the SQG equation. *Comm. Pure Appl. Math.*, 72(9): 1809–1874, 2019.

Cao, J., Li, B., Wu, Y. and Yao, F. Computing rough solutions of the KdV equation below L^2. Preprint, arXiv:2506.21969, 2025.

Cheng, X. Energy stable semi-implicit schemes for the 2D Allen-Cahn and fractional Cahn-Hilliard equations, *IMA J. Numer. Anal.*, 46(2): 758–794, 2026.

Cheng, X., Luo, Z. and Wang, S. Stability and convergence of an iterative low-regularity method for the Cahn–Hilliard equation. *J. Differential Equations*, 478: 114622, 2026a.

Cheng, X., Kwon, H. and Li, D. Non-uniqueness of stationary weak solutions to the surface quasi-geostrophic equations. *Comm. Math. Phys.*, 388(3): 1281–1295, 2021.

Cheng, X., Luo, Z. and Wang, S. On semi-implicit schemes for the incompressible Euler equations via the vanishing viscosity limit, preprint, arXiv:2406.12320, 2024a.

Cheng, X., Luo, Z. and Wang, S. The vanishing viscosity limit of the surface quasi-geostrophic equations in borderline Besov spaces: Rates and same topology convergence, preprint, 2026b.

Cheng, X., Luo, Z., Yang, Z. and Yuan, C. Global well-posedness and uniform-in-time vanishing damping limit for the inviscid Oldroyd-B model, preprint, arXiv:2410.09340, 2024b.

Chorin, A. J. Numerical solution of the Navier–Stokes equations. *Math. Comput.*, 22, 745–762, 1968.

Chorin, A. J. On the convergence of discrete approximations to the Navier–Stokes equations. *Math. Comput.*, 23, 341–353, 1969.

Constantin, P., Lai, M. C., Sharma, R., Tseng, Y. H. and Wu, J. New Numerical Results for the Surface Quasi-Geostrophic Equation. *J Sci. Comput.* 50: 1–28, 2012.

Constantin, P., Majda, A. J. and Tabak, E. Formation of strong fronts in the 2-D quasi-geostrophic thermal active scalar. *Nonlinearity*, 7(6): 1495–1533, 1994.

Constantin, P. and Nguyen, H. Q. Global weak solutions for SQG in bounded domains. *Comm. Pure Appl. Math.*, 71(11): 2323–2333, 2018.

Constantin, P. and Wu, J. Behavior of solutions of 2D quasi-geostrophic equations. *SIAM J. Math. Anal.*, 30(5): 937–948, 1999.

E, W. and Liu, J. Projection method I: convergence and numerical boundary layers. *SIAM journal on numerical analysis*, 1017-1057, 1995.

Guo, B. and Zou, J. Fourier spectral projection method and nonlinear convergence analysis for Navier–Stokes equations. *Journal of mathematical analysis and applications*, 282(2): 766-791, 2003.

Han, J., Jentzen, A. and E, W. Solving high-dimensional partial differential equations using deep learning, *Proc. Natl. Acad. Sci. U.S.A.* 115(34): 8505-8510, 2018.

He, Y. Euler implicit/explicit iterative scheme for the stationary Navier–Stokes equations. *Numer. Math.*, 123, 67–96, 2013.

Held, I. M., Pierrehumbert, R. T., Garner, S. T. and Swanson, K. L. Surface quasi-geostrophic dynamics. *J. Fluid Mech.*, 282:1-20, 1995.

Heywood, J. G. and Rannacher, R. Finite element approximation of the nonstationary Navier–Stokes problem. I. Regularity of solutions and second-order spatial discretization. *SIAM J. Numer. Anal.*, 19, 275–311, 1982.

Heywood, J. G. and Rannacher, R. Finite-element approximation of the nonstationary Navier–Stokes problem part IV: error analysis for second-order time discretization. *SIAM J. Numer. Anal.*, 27, 353–384, 1990.

Hill, A. T. and Süli, E. Approximation of the global attractor for the incompressible Navier- Stokes equations, *IMA J. Numer. Anal.*, 20: 633–667, 2000.

Hou, T. Y. and Wetton, B. Second-Order Convergence of a Projection Scheme for the Incompressible Navier–Stokes Equations with Boundaries, *SIAM Journal on Numerical Analysis*, 30(3): 609–629, 1993.

Isett, P. and Ma, A. A direct approach to nonuniqueness and failure of compactness for the SQG equation. *Nonlinearity*, 34(5): 3122–3162, 2021.

Kiselev, A., Nazarov, F. and Volberg, A. Global well-posedness for the critical 2D dissipative quasi-geostrophic equation. *Invent. Math.*, 167(3): 445–453, 2007.

Li, B., Ma, S. and Schratz, K. A Semi-implicit Exponential Low-Regularity Integrator for the Navier–Stokes Equations. *SIAM J. Numer. Anal.*, 60(4): 2273-2292, 2022.

Li, D. On Kato–Ponce and fractional Leibniz. *Rev. Mat. Iberoam.*, 35(1): 23–100, 2019.

Marchand, F. Existence and regularity of weak solutions to the quasi-geostrophic equations in the spaces L^p or $\dot{H}^{-\frac{1}{2}}$, *Comm. Math. Phys.*, 277(1): 45–67, 2008.

Onsager, L. Statistical hydrodynamics. *Nuovo Cimento (9)*, 6 Supplemento (2 (Convegno Internazionale di Meccanica Statistica)):279–287, 1949.

Pedlosky, J. *Geophysical fluid dynamics*. Springer, New York, 1982.

Resnick, S. G. Dynamical problems in non-linear advective partial differential equations, Ph.D. thesis, University of Chicago, 1995, available at https://www.proquest.com/docview/304242616.

Rousset, F. and Schratz, K. A general framework of low regularity integrators, *SIAM J. Numer. Anal.*, 59(3): 1735–1768, 2021.

Süli, E. Convergence and non-linear stability of the Lagrange–Galerkin method for the Navier–Stokes equations. *Numer. Math.*, 53, 459–483, 1988.

Wetton, B. Finite difference vorticity methods. *The Navier-Stokes Equations II—Theory and Numerical Methods: Proceedings of a Conference held in Oberwolfach, Germany, August 18–24, 1991.* Berlin, Heidelberg: Springer Berlin Heidelberg, 210-225, 2006.

Wu, Y. and Zhao, X. Optimal convergence of a second order low-regularity integrator for the KdV equation. *IMA J. Numer. Anal.*, 42(4): 3499–3528, 2022.

X. Cheng, Research Institute of Intelligent Complex Systems, Fudan University, Shanghai, P.R. China
Email address: xycheng@fudan.edu.cn

Z. Luo, School of Science, Shenzhen Campus of Sun Yat-sen University, Shenzhen, P.R. China
Email address: luozhn7@mail.sysu.edu.cn

S. Wang, School of Mathematical Sciences, Peking University, Beijing, P.R. China
Email address: everest_sheng@pku.edu.cn